

ACTIVE STABILIZATION TECHNIQUE OF DYNAMIC MACHINING SYSTEM
DURING BORING

A Thesis Submitted

In Partial Fulfilment of the Requirements

for the Degree of

MASTER OF TECHNOLOGY

by

SHYAMAL CHATTERJEE

to the

DEPARTMENT OF MECHANICAL ENGINEERING

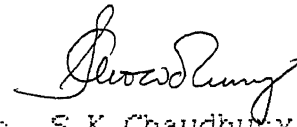
INDIAN INSTITUTE OF TECHNOLOGY

KANPUR

CERTIFICATE

This is to certify that the thesis entitled 'ACTIVE STABILIZATION
TECHNIQUE OF DYNAMIC MACHINING SYSTEM DURING BORING ' by
chatterjee,Shyamal ,roll no. 8910533 , is a record of work carried
out under my supervision and has not been submitted elsewhere for
a degree.

March ,1991.



Dr. S.K. Chaudhury

Assistant Professor

Department of Mechanical Engineering

Indian Institute of Technology

Kanpur

26 MAY 1991

CENTRAL LIBRARY

1000 PAGE 2

Acc. No. A112177

ME-1991-M-CHA-ACT

DEDICATED TO

MY NATION

ACKNOWLEDGEMENT

I would like to express my heartfelt gratitude to Dr. S.K. chaudhury for his invaluable guidance during the course of this work.

I would like to thank Mr. B.P.Bhartiya for rendering his service whenever needed. My thanks are due to Mr. M.M singh and Dr.N.vays of vibration Lab. for extending the laboratory facilities whenever needed.

My sincere thanks are due to all my friends for their timely help.

Finally I specially thank Mr. Rajpal and Mr. Chauhan of ACES lab for their invaluable help and suggestions regarding electrical circuits.

CONTENTS

CHAPTER -I	1
1.1 INTRODUCTION	2
1.2 REVIEW OF THE PREVIOUS WORKS	8
1.3 OBJECTIVES OF THE PRESENT WORK	8
CHAPTER -II	
MATHEMATICAL MODELING OF THE SYSTEMS	
2.1 MODELING OF THE UNCONTROLLED SYSTEM : MODEL -1	11
2.1a DETERMINATION OF G_c [DIRECT HARMONIC RESPONSE FUNCTION OF THE BORING BAR AT THE TIP i.e. NEAR CUTTING EDGE]	12
2.2 MODELING OF DISPLACEMENT FEED-BACK CONTROL SYSTEM : MODEL-2	15
2.2a DETERMINATION OF G_{et} [CROSS RESPONSE FUNCTION BETWEEN THE EXCITER POSITION AND THE TIP OF THE BORING BAR]	16
2.2b DYNAMICS OF THE EXCITER: DETERMINATION OF G_e	16
2.3 MODELING OF THE ACCELERATION FEED-BACK CONTROL SYSTEM: MODEL-3	21
2.4 MODELING OF THE FORCE FEED-BACK CONTROL SYSTEM : MODEL-4	21
2.5 SIMULATION STUDIES OF THE PROPOSED MODELS	22
2.5a STABILITY CRITERION	23
2.5b SIMULATION OF MODEL-1	24
2.5c SIMULATION OF MODEL-2	25
2.5d SIMULATION OF MODEL-3	26
2.5e SIMULATION OF MODEL-4	27
2.6 RESULTS AND DISCUSSION : COMPARISON OF THE MODELS	28
CHAPTER-III	
DESIGN AND CALIBRATION OF THE EXPERIMENTAL SET-UP	
3.1 AN OVERALL DESCRIPTION OF THE EXPERIMENTAL SET-UP	44
3.2 DESIGN OF THE EXCITER	45
3.3 DESIGN CRITERION OF THE EXCITER	46
3.4 CALIBRATION OF THE EXCITER	47
CHAPTER-IV	
EXPERIMENTAL RESULTS AND DISCUSSION	
4.1 EXPERIMENTAL PROCEDURE AND RESULTS	57
4.2 CONCLUSION	57
4.3 SCOPE OF THE FUTURE WORK	59
APPENDIX-A	
APPENDIX-B	
APPENDIX-C & D	

LIST OF FIGURES

FIG. NO.	TITLE	PAGE
Fig. 2.1	Block diagram of uncontrolled cutting	30
Fig. 2.2	Block diagram of displacement feed-back control system	31
Fig. 2.3	Arrangement of electromagnets in the exciter	32
Fig. 2.4	Equivalent circuit diagram of magnetic coil	33
Fig. 2.5	Block diagram of acceleration feed-back control system	34
Fig. 2.6	Block diagram of force feed-back control system	35
Fig. 2.7	Regeneration spectrum of the uncontrolled system	36
Fig. 2.8	Regeneration spectrum of the displacement feed-back control system	37
Fig. 2.9	Regeneration spectrum of the acceleration feed-back system	38
Fig. 2.10	Regeneration spectrum of the force feed-back control system	39
Fig. 2.11	Gain sensitivity plot of acceleration feed-back system	40
Fig. 2.12	Gain sensitivity of displacement feed-back system	41
Fig. 2.13	Gain sensitivity of the force feed-back system	42
Fig. 2.14	Stability chart	43
fig. 3.1	Schematic diagram of the experimental set-up	49
Fig. 3.2	Schematic diagram of the boring bar	50
Fig. 3.3, 3.4	schematic diagram of the exciter	51-52
Fig. 3.5	Effect of no. of turns of coil on stability	53
Fig. 3.6	frequency response curve of the exciter	54
Fig. 3.7	Voltage response curves of the exciter	55
Fig. 4.1-4.14	Vibration pattern of the boring bar during controlled and uncontrolled cutting	63-70
Fig. 4.15	Hysteresis loop of the ferromagnetic material under alternating field consisting of two different frequencies	71
Fig. 4.16	Suggested circuit diagram of the magnetic coil for improved response of the exciter	72
Fig. A-1	Tulstys model of two degrees of freedom,	A-4

Fig. A-2	co-ordinate transformation diagram	A-4
Fig. B-1	Nonlinear behavior of magnetization	B7
Fig. B-2	Nonlinear relation of current and flux	B7
Fig. B-3	effect of nonlinearity of magnetization on current	B8
Fig. B-4	Linearization of magnetization ,by biasing	B8
Fig. B-5	Dependence of inductance on D.C biasing	B8
Fig. B-6	Existance of minor hysteresis loops	B9
Fig. B-7	Hysteresis and after effect	B9
Fig. B-8	Anhysteresis	

NOMENCLATURE

$A \text{ (cm}^2\text{)} =$ cross-sectional area of the bar

$A_c \text{ (cm}^2\text{)} =$ cross sectional area of the magnetic core

$E \text{ (kg/cm}^2\text{)} =$ elastic modulus of boring bar material

$F_0 \text{ (kg)} =$ static cutting force in the thrust direction

$F(t), F(s) =$ instantaneous cutting force in the thrust direction in time and laplace domain respectively .

$dF_1(t) , dF_1(s) =$ dynamic force associated with change in chipthickness in time and laplace domain respectively

$dF_2(s) =$ dynamic force component due to penetration resistance

$f(t) =$ resultant cutting force

$f_e(t) , F_e(s) =$ excitation force in time and laplace domain respectively

$g \text{ (cm/sec}^2\text{)} =$ acceleration due to gravity

$G_t(s) =$ direct harmonic response function of the boring bar at the tip

$G_e(s) =$ transfer function of the exciter

$G_{et}(s) =$ transfer function describing the dynamics of the boring bar from exciter position to the tip

$I \text{ (cm}^4\text{)} =$ area moment of inertia of the boring bar cross-section

$i_1(t), I_1(s) \text{ (amp.)} =$ current

$j = \sqrt{-1}$

$\bar{K} =$ feed back path amplifier gain

$K_c \text{ (kg/cm)} =$ cutting stiffness in thrust direction

$K_d \text{ (kg.sec/cm)} =$ penetration coefficient in thrust direction

$l \text{ (cm)} =$ length of the boring bar

L_e = distance of the exciter from the tool-base

L_{ii} (henry) = inductance of magnetic coils

l_c (cm) = length of the magnetic core

M, M_0 = mutual inductances

N = No. of turn of the magnetic coil

N_0 = rpm of the spindle

$R(\Omega)$ = resistance of the magnetic coil

T (sec.) = time period for single revolution of the workpiece

$u(t), U(s)$ = instantaneous chip thickness in time domain and laplace domain respectively

$\delta u(t), \delta U(s)$ = dynamic change in chip thickness

w_i (rad/sec) = i th natural frequency of the boring bar

w = frequency

$X_j(x)$ = shape function of the cantilever beam for the j -th mode of vibration.

$y(t), Y(s)$ = dynamic displacement of boring bar at the tip

$Y_c(s)$ = controlled dynamic displacement of the tip of the boring bar in laplace domain

$Y_{ft}(s)$ = displacement of the tip due to excitation at the exciter position. in laplace domain

$\ddot{Y}(s), \ddot{Y}_c(s)$ = acceleration in laplace domain

α_0 = chatter growth exponent

β = angle made by the resultant cutting force with the m/c bed

γ (kg/cm³) = specific weight of the boring bar material

ω_0, ω_1 = gap between the magnets

$\phi_j(t)$ = certain time function for the j th mode of vibration of the cantilever beam.

μ = overlap factor

μ_0 (weber/amp.m) = permeability of the vacuum

$F_{st}(s)$ = short term disturbing force

CHAPTER I

1.1 Introduction:

In the modern rocket-age machining technology aims at achieving two primary goals-one is high production rate and another high accuracy and finish. There are many causes which are playing adversely against achieving these objectives. Chatter is one of the most unpredictable evils which fall in this category. Since 1948 many researchers attempted to investigate into the mechanism of chatter and so far a considerable amount of knowledge has been gathered in this field. However, whatever may be the cause of chatter, the main objectives of the present researchers is to eliminate it in order to counteract its detrimental effect on the surface-finish and accuracy. As far as chatter control technique is concerned many of them have been found to fight the chatter out.

So far two principal reasons have been detected to be the cause of chatter. Regeneration effect and mode-coupling effect are those two which may occur solely or simultaneously. Besides, many other effects, such as primary chatter due to the velocity dependent friction etc., may lead to chatter. But according to the degree of severity regenerative chatter is most important. Chatter is nothing but the unstable vibration of machine during machining operation. Explicitly speaking if steady state cutting condition is disturbed somehow, due to the nature of cutting process itself the elastic system of the machine tool may be thrown into vibration the amplitude of which theoretically grows up gradually till the breakage of tool. Actually due to nonlinearity in the elastic

system at higher amplitude, vibration level becomes constant after a certain time. Thus, chatter is different from forced and free vibration of the machine tools and cannot be predicted beforehand. Obviously in the design stage of machine tools very little measure can be taken against chatter. Chatter is mostly related to the cutting process which itself is a random phenomenon with minute oscillation of force, depth of cut, feed etc. due to the anisotropic behavior of the workpiece material and many other reasons.

It is sometimes useful to include proper damping and stiffness in the weak parts susceptible to chatter. But the technique being passive, can not adapt itself to the inconsistent change in system behavior. Perhaps an on-line control system should be the best in dealing chatter due to its capability of taking the randomness of the process in full consideration with the help of continuous monitoring and correcting device of the system response.

Furthermore chatter is generally not a great concern during rough cutting operation. Only during finishing operations chatter must be eliminated in order to ensure a good surface finish.

In the following article some of the recent active control techniques to reduce chatter have been discussed.

1.2 Review of the previous works:

B. R. MacMANUS [1] introduced a new technique of providing positive damping in the cutting process itself through dynamic heating to eliminate chatter. It was distinctive in nature with respect to the trend of introducing damping in machine tool structure. An alternating current was generated from the electrical signal from

the displacement monitoring transducer(measuring the relative displacement between the tool and workpiece)and this current was used for dynamic heating of the workpiece.The frequency of dynamic heat supply matched the frequency of chatter with proper phasing and rectification.Besides ,a steady component of heat was also applied.The closed loop response of the system showed progressive reduction in amplitude with increasing feed-back gain.Measurements of stabilization characteristics proved the interdependence of maximum current required for stabilization and phase of dynamic heat oscillation with respect to the tool vibration.The utility index had been defined to be the maximum current and its minimization was of importance.The basic mechanism of the closed loop stabilization technique is the superimposition of a force oscillation(due to thermally induced shear-angle variation and periodic variation of the shear strength of the metal) on the dynamic force variation due to non-steady cutting process, with a proper relative phase.

T.R.COMSTOCK ,F.S.TSE and J.R.LEMON [2] developed a feed-back control loop that instantaneously controlled the tool-work relative displacement.In CMI[CONTROLLED MECHANICAL IMPEDANCE] technique the relative vibration between tool and workpiece was sensed and fed back through a differential amplifier ,controller and servo valve to actuate a hydraulic actuator for properly positioning the tool with respect to the workpiece.They made the following analytical conclusions:

1. CMI can improve stability of the single point cutting process
- 2.If servo valve natural frequency(ω_v) is less than that of

machine(w_m) or they match ,the CMI process fails.

3. For a given value of (w_v/w_m) ,(k_l/w_v)=0.9 is the optimum point, k_l being loop gain. Greater the value of (w_v/w_m) for a given (k_l/w_v) ,greater the improvement in stability. As (k_l/w_v) approaches 2.0 ,the servo positioning loop becomes unstable.

4. Experimentally they showed that with the CMI application 35 times improvement in stability (represented by the value of (k_c/k_m), k_c being cutting stiffness, k_m static stiffness of the structure) can be achieved.

C.L.NACHTIGAL and N.H.COOK [3] used the similar technique .Sensing the force variation and feeding the signal through control network to an electrohydraulic-tool-servo system they improved the stability condition during cutting.They provided a basis for designing the control system for optimum performance.The following design objectives were fulfilled:

- 1.Increased M.R.R with improved stability.
- 2.Better transient response to disturbance.
- 3.Increase in apparent static stiffness of the system, and thereby, improvement in the system's tolerance capability.
- 4.Suppression of input forcing functions such as spindle imbalance ,foundation vibration etc.

The cutting force was selected as the measured variable because of its certain advantages over displacement measurement scheme -such as:

1. The force transducer is isolated from severe cutting zone environment.
- 2.Cutting force is not dependent on workpiece geometry.
- 3.once the force transducer is calibrated it can be used for

any material and geometry.

Two different actuator locations were considered:

1. Within the loop established by machine-tool-workpiece
2. At some point on the machine structure outside the previously mentioned loop.

In view of the design requirement that the active control system must be capable of increasing the static stiffness, the actuator had to be placed in series within the cutting force loop.

Because of the unknown variability in the dynamics of the machine-tool system, the controller parameters were chosen to accommodate some mismatch between structure and tool servo dynamics.

L.P. BEILIN et al [4] suggested the transfer functions for the principal units in systems for stabilizing the force parameter during cutting and gave specific recommendations on choosing the type and design of regulator with the information on cutting frequency, phase, amplitude. The stabilization procedure was controlling the feed. But he felt about the need of a two-channel system where the first channel ensures the stabilization of the force parameter under static conditions whilst the second stabilizes this parameter during sudden changes in load. An optimization procedure for calculating the optimum signal input to the feed-drive controller was also provided.

M.S. GORODETSKII et. al [5] discussed about the adaptive control systems for stabilizing the force parameter by controlling the feed. He showed that the problem of producing a stable system with a small static error when gain of the cutting-process can change widely, can be solved by:

1. producing a static regulation system with high gain ,
2. introducing a nonlinear element into the static system regulator and
3. by producing an astatic system to ensure zero error for any value of regulator gain.

He took into considerations different constraints of feed ,power and voltage to control feed-drive. He discussed about different dynamic and static characteristics of the system in different cutting conditions.

R.G.KLEIN.and C.L.NACHTIGAL [6] attempted to control the boring bar chatter.They introduced a theoretical basis for active control system. Their analysis includes the practical consideration of principal modes in boring bar model.A response function of the boring bar subject to dynamic cutting force is also given.The state variable used as the control signal is cutting force which contains static as well as dynamic information.They considered that due to the large length-to-diameter ratio of the boring bar the torsional and bending frequency are widely separated and are uncoupled.Slope control actuation at the base of the bar is used .The control signal is conditioned through an analog controller which in turn drives an electrohydraulic position servo ;the servo being connected to the bar could provide a slope control input.

Simulation of the control system model gives the following results:

- 1.The control system has infinite static stiffness.
- 2.The maximum dynamic gain of the controlled system is less than that of the uncontrolled system indicating less

susceptibility to chatter for the same cutting stiffness.

3. The control system has a greater minimum real part which indicates that machining rates are possible under stable cutting conditions.

It was found that the experimental [7] boring bar set-up did exhibit two principal modes but the controller could be designed independently of these modes. Cutting tests were performed using derlin plastic on a lathe equipped with a pivoted boring bar, which was being controlled by electrohydraulic servo. It was found that the theory established did in fact predict qualitatively the new stability borderline. Width of cut was improved by a factor of twelve and equivalent static stiffness was increased without bound.

TOMIO MATSUBARA, HISATAKA YAMAMOTO and HIROSHI MIZUMOTO [8] made a comparative study of the effect of mode-coupling and regeneration on chatter stability. The results obtained are as follows:

1. Chatter stability limits evaluated by the theory of regenerative effect are lower than those obtained by the theory of mode-coupling in any condition.

2. As experimental results agree well with the stability limits of the regenerative chatter vibration, it can be concluded that boring bar chatter is dominated by regeneration.

3. It becomes clear that the side cut boring bar can hardly impart any marked improvement on chatter stability.

1.3 OBJECTIVES OF THE PRESENT WORK:

The present work is in the field of on-line control of machine tool chatter. Boring operation often encounters severe vibration due to its long overhang ie less static stiffness. In the past much attention has been given on improving the boring bar dynamics during cutting. Most of them are passive in nature and very little has been done to suppress the chatter actively. Increasing damping and rigidity can help in reducing vibration of boring bar, but those being passive in nature can't deal perfectly with the randomness of the dynamic cutting force. An on-line or active control is preferred in this respect, as it is capable of taking the randomness in vibration pattern. So far many state variables, such as force, relative displacement etc., have been selected for the active control during turning, boring etc. In almost all the cases electrohydraulic servo is used as an actuator. Though electrohydraulic servo can give sufficiently good results, its high cost should make the researchers investigate into an alternative actuator which will be of low cost. An electromagnetic exciter may replace an electrohydraulic actuator as far as cost is considered. Thus the potentialities of an electromagnetic exciter in controlling the chatter should be a matter of investigation. Furthermore, no comparative studies between the use of different state variables exist.

The objectives of the present work are as follows:

1. Mathematical modeling of the uncontrolled and controlled cutting systems.

Controlled systems using displacement, acceleration and force

monitoring transducer are to be compared theoretically.

2.Design of an electromagnetic exciter and making a theoretical analysis of its dynamics.

3.Design of a feed-back control system for the stability of boring operation. The control action is based on the following principle: sensing of a state variable pattern of the boring bar during machining with a transducer and this signal ,after appropriate amplification is to be back to the electromagnetic exciter with an opposite phase.

4.Experimental verification of the proposed control system model in real time machining.

CHAPTER II

MATHEMATICAL MODELING OF THE SYSTEMS

So far many research workers have attempted to control boring bar chatter. In most of the situations the workpiece was taken to be rigid and systems were designed to combat chatter arising out of mode-coupling and/or regenerative effect. In the present work initially those principles have been followed except the mode-coupling effect which is less serious in comparison to regenerative effect. Less attention may be paid to mode-coupling because of the consequence of the research carried out by *TOMIO MATSUBARA*, *HISATAKA YAMAMOTO* and *HIROSHII MIZUMOTO* [8]. They Proved both analytically and experimentally that stability limit calculated by regenerative chatter theory is lower than that obtained by the mode-coupling theory at any condition. By stability limit they meant the value of real part of the minimum dynamic compliance of the elastic system under unsteady cutting condition. Though the occurrence of coupled oscillation in all situations can't be ensured, but it can easily be suppressed, if it occurs, at least to acceptable degree by properly orienting the boring bar. Thus, any system designed to control regenerative chatter will be the most effective one and is expected to control any other types of chatter.

As discussed in the literature review, so far electrohydraulic servo has been widely used in chatter control circuits. But the need of further investigation into the propensity of electromagnetic exciter in chatter control system is obvious due to its low cost compared to above mentioned electrohydraulic servo. In the present chapter the uncontrolled and controlled

system regarding chatter will be modeled and simulated keeping in view the stability of the dynamics of cutting and its interaction with the elastic system of the tool. the relative advantages and disadvantages of the use of different state variables will also be discussed.

2.1 MODELING OF UNCONTROLLED SYSTEM: MODEL-1

The present modeling is based on the assumptions that the workpiece is absolutely rigid and does not deflect under cutting force, where as the tool is non-rigid, responding solely to the dynamic cutting force.

The well known equation representing the dynamic cutting force is given by

$$F(t) = F_0 + dF(t) \quad (1)$$

where dF is small oscillation of cutting force (in thrust direction) arising out of some short term disturbances which are impulsive in nature and F_0 is the static cutting force component in thrust direction. Their action on the depth of cut variation is indirect. First the cutting force is affected and subsequently causes a change in depth of cut. Conventionally the instantaneous chip thickness is given by the following relation

$$u(t) = u_0 - [y(t) - \mu y(t-T)] \quad (2)$$

$y(t)$ being displacement of boring bar under dynamic cutting force in the chip thickness direction, μ being overlap factor, T is time taken by the workpiece for single revolution, u_0 is uncut chip thickness.

Variation in depth of cut, thus, is written to be

$$\delta u(t) = u(t) - u_0 \quad (3)$$

$$\text{or} \quad \delta u(t) = - [y(t) - \mu \cdot y(t-T)] \quad (4)$$

transforming equation (4) in the Laplace domain (in relaxed condition) one gets

$$\delta U(s) = - Y(s) \cdot [1 - \mu \cdot e^{-T \cdot s}] \quad (5)$$

Thrust force associated with change in chip thickness is given by

$$dF_1(s) = - K_c \cdot Y(s) \cdot [1 - \mu \cdot e^{-T \cdot s}] \quad (6)$$

and force due to penetration resistance is as follows

$$dF_2(s) = -K_d \cdot s \cdot Y(s) \quad (7)$$

K_c being cutting stiffness in chip thickness direction, K_d is penetration coefficient.

Thus, change in dynamic force is

$$\begin{aligned} dF(s) &= dF_1(s) + dF_2(s) \\ &= - K_c \cdot [1 - \mu \cdot e^{-T \cdot s}] - K_d \cdot s \cdot Y(s) \\ &= - Y(s) \cdot [K_c \cdot (1 - \mu \cdot e^{-T \cdot s}) + K_d \cdot s] \end{aligned} \quad (8)$$

The block diagram representing the interaction of elastic system and cutting process is shown in the fig.[2.1]. In the diagram G_t is the direct response function of the tool under cutting force at tool tip. The analytical expression for G_t can be obtained as follows.

2.1a Determination of G_t :

The boring bar can be assumed to be a cantilever beam responding to the variable cutting force in the following way

$$y(t) = \sum_{j=1,2,3,\dots} \phi_j(t) \cdot X_j(x) \quad (9)$$

Where $X_j(x)$ = Shape function or normal function for cantilever beam for it's j th mode of vibration

and $\phi_j(t)$ is certain time function and may be obtained through the following equation

$$\ddot{\phi}_1 + \left[\frac{a^2}{l^4} \lambda_1^4 \right] \cdot \phi_1 = \left[\frac{F(t) \cdot g}{A \cdot \gamma \cdot l} \right] \cdot (X_1) \big|_{x=L} \quad (10)$$

for a force $F(t)$ acting on the boring bar of length l , at a distance L from the fixed end ;

$$\text{where } a^2 = \frac{E \cdot I \cdot g}{A \cdot \gamma}$$

As it has been discussed that coupled oscillation is less serious compared to regeneration and can be avoided by proper designing [Appendix-A] it's effect has not been taken into consideration. Only modes in the chip thickness direction will be considered.

$$X_1 = \cosh(f(x)) - \cos(f(x)) - \sigma_1 \left[\sinh(f(x)) - \sin(f(x)) \right] \quad (11)$$

$$\text{where } f(x) = \frac{\lambda_1 \cdot x}{l} \quad (12)$$

x being the co-ordinate axis along the length of the boring bar.

If the modes are widely separated the higher modes can conveniently be neglected without seriously affecting the result, particularly in the chatter phenomenon, where in most of the cases first or principal mode gets excited.

For first mode of vibration of the cantilever $\sigma_1 = 0.73409$ and $\lambda_1 = 1.875$

Transforming equation (10) into complex domain we get .

$$\phi_1(s) \left[s^2 + \frac{a^2 \cdot \lambda_1^4}{I^4} \right] = F(s) \cdot \frac{q}{A \cdot \gamma \cdot I} (X_1) \Big|_{x=L} \quad (13)$$

Considering damping in the system equation (13) takes the following form

$$\phi_1(s) \left[s^2 + \frac{A \cdot \gamma \cdot I}{g} D \cdot s + \frac{a^2 \cdot \lambda_1^4}{I^4} \right] = F(s) \cdot \frac{q}{A \cdot \gamma \cdot I} (X_1) \Big|_{x=L} \quad (14)$$

where D is the damping per unit mass of the boring bar.

$$\text{Thus } Y(s, x) = \phi_1 \cdot x_1 \quad (15)$$

It can be shown that

$$\omega_1^2 = \frac{a^2 \cdot \lambda_1^4}{I^4} \quad (16)$$

$$\text{and } \frac{A \cdot \gamma \cdot I^5 \cdot D}{g \cdot a^2 \cdot \lambda_1^4} = \frac{2 \cdot \xi_1}{\omega_1^2} \quad (17)$$

Thus

$$G_t(s) = \frac{Y(s, 1)}{F(s, 1)} = \frac{\frac{(X_1)_{x=1} \cdot (X_1)_{x=1}}{\left[\frac{s^2}{\omega_1^2} + \frac{2 \cdot \xi_1 \cdot s}{\omega_1} + 1 \right]}}{\frac{q}{A \cdot \gamma \cdot I}} \cdot EQS_1 \quad (18)$$

$$\text{where } EQS_1 = \frac{E \cdot I \cdot \lambda_1^4}{I^3} \quad (19)$$

2.2 MODELING OF PROPOSED CONTROL SYSTEMS: MODEL-2

The main problem of control is to select an appropriate state variable (quantity to be monitored). The sensing of relative displacement between the tool and the workpiece should be the best in this regard, as the corresponding signal is capable of providing the information about the static and dynamic deflection both. Though during boring the positioning of the displacement sensor into the bore is not very easy, still technological contributions to the small size of the sensor may get rid of this restriction. In this model position measuring sensor has been tried.

Relative displacement between the tool and the workpiece is measured in the chip thickness direction and the signal is fed back through an amplifier circuit into the electromagnetic exciter; in the way the phase of the signal has been inverted. Intuitively speaking two out of phase vibration may counteract resulting in reduced vibration level.

The complete block diagram of the control system is shown in the fig. [2.2]

Dynamic gain of the transducer and the amplifier circuit can be multiplied and expressed in the form of a constant K . G_e transfers the signal to the force in the exciter. G_{et} is the transfer function describing the dynamics from the exciter position to the cutting edge at the tip of the bar. The exciter, due to its large size, can expediently be placed near the base of the bar, rather than at the tip.

2.2a Determination of G_{et} :

G_{et} describes the dynamics of the boring bar and can be expressed as

$$G_{et} = \frac{Y_{ft}(s)}{F_e(s)},$$

where $Y_{ft}(s)$ is the displacement at the bar tip due to excitation at the exciter position with the exciter force $F_e(s)$, in the complex domain.

The rest of the procedure is same as the derivation of G_t . The only difference is that the excitation point and the point where the displacement is to be measured are different.

Thus,

$$G_{et} = \frac{X_1^{(x=1)} e^{-(X_1^{(x=1)})}}{\text{EQS.} \left[\frac{s^2}{w_1^2} + \frac{2 \cdot \xi_1 \cdot s}{w_1} + 1 \right]} \quad (20)$$

2.2b Dynamics of the exciter: determination of G_e

The exciter is of electromagnetic type, consisting of two permanent electromagnets (1 & 3) and another electromagnet (2) being fed with an a.c. signal, as shown in the fig. [2.3]. Two permanent electromagnets are fixed rigidly and the other one is free to move.

A generalized treatment of multiple excitation [11] :

Three coils are supplied with current i_i at the voltage v_i . Coils have SELF INDUCTANCE L_{ii} and MUTUAL INDUCTANCES M & M_0 . $y_e(t)$ & $f_e(t)$ are the displacement and the excitation force respectively.

Voltage equations are as follow:

$$\left. \begin{aligned} v_1 &= R_1 \cdot i_1 + \frac{d}{dt}(L_{11} \cdot i_1) + \frac{d}{dt}(M \cdot i_2) \\ v_2 &= R_2 \cdot i_2 + \frac{d}{dt}(L_{22} \cdot i_2) + \frac{d}{dt}(M \cdot i_1 + M_0 \cdot i_3) \\ v_3 &= R_3 \cdot i_3 + \frac{d}{dt}(L_{33} \cdot i_3) + \frac{d}{dt}(M_0 \cdot i_2) \end{aligned} \right\} \quad (21)$$

Electrical energy input in time dt

$$\begin{aligned} &= (R_1 \cdot i_1^2 + R_2 \cdot i_2^2 + R_3 \cdot i_3^2) + \\ &(i_1^2 \cdot dL_{11} + i_2^2 \cdot dL_{22} + i_3^2 \cdot dL_{33}) + 2 \cdot i_1 \cdot i_2 \cdot dM + 2 \cdot i_2 \cdot i_3 \cdot dM_0 + \\ &(L_{11} \cdot i_1 + M \cdot i_2) \cdot di_1 + (L_{22} \cdot i_2 + M \cdot i_1 + M_0 \cdot i_3) \cdot di_2 + \\ &\quad (L_{33} \cdot i_3 + M \cdot i_1 + M_0 \cdot i_2) \cdot di_3 \end{aligned} \quad (22)$$

Field storage is given by

$$\begin{aligned} &d \left[\frac{1}{2} \cdot L_{11} \cdot i_1^2 + \frac{1}{2} \cdot L_{22} \cdot i_2^2 + \frac{1}{2} \cdot L_{33} \cdot i_3^2 \right] \\ &= \frac{1}{2} \left[i_1^2 \cdot dL_{11} + i_2^2 \cdot dL_{22} + i_3^2 \cdot dL_{33} \right] + i_1 \cdot i_2 \cdot dM + i_2 \cdot i_3 \cdot dM_0 + \\ &(L_{11} \cdot i_1 + M \cdot i_2) \cdot di_1 + (L_{22} \cdot i_2 + M \cdot i_1 + M_0 \cdot i_3) \cdot di_2 \\ &\quad + (L_{33} \cdot i_3 + M \cdot i_1 + M_0 \cdot i_2) \cdot di_3 \end{aligned} \quad (22)$$

Energy balance equation:

Mechanical input + Electrical input = Mech. storage + field storage + heat.

or , - Mechanical input + Mechanical storage + Heat = Electrical input - Field storage

$$\text{or , Mechanical energy output + Heat} = \sum R_i i_i^2 = \frac{1}{2} \left[i_1^2 dL_{11} + i_2^2 dL_{22} + i_3^2 dL_{33} \right] + i_1 i_2 dM + i_2 i_3 dM_0$$

$$\text{or , } f_e dy_e = \frac{1}{2} \left[i_1^2 dL_{11} + i_2^2 dL_{22} + i_3^2 dL_{33} \right] + i_1 i_2 dM + i_2 i_3 dM_0 \quad (23)$$

$$\text{as , heat} = \sum R_i i_i^2$$

Now if $i_1 = i_3$

$$f_e = \frac{1}{2} i_1^2 \left[\frac{d}{dy_e} (L_{11} + L_{33}) \right] + \frac{1}{2} i_2^2 \cdot \frac{d}{dy_e} (L_{22}) + i_1 i_2 \cdot \frac{dM}{dy_e} + i_2 i_3 \cdot \frac{d}{dy_e} (M_0) \quad (24)$$

Change in $(L_{11} + L_{33})$ for a change in x is zero, as L_{11} & L_{33} changes by same amount but opposite in sign. Similarly L_{22} is also invariant to x .

$$\text{Now } dy_e = -d\omega_1 = d\omega_0$$

$$\text{and } M = - \frac{\mu_0 \cdot N^2 \cdot A_c}{\omega_0}$$

$$\text{and } M_0 = \frac{\mu_0 \cdot N^2 \cdot A_c}{\omega_1}$$

where A_c = area of the core

ω_1, ω_0 = gap between the magnets

N = no. of turns in the magnets

μ_0 = Magnetic permeability in the air

$$\frac{dM}{dy_e} = \frac{dM}{d\omega_0} \cdot \frac{d\omega_0}{dy_e} = \frac{\mu_0 \cdot N^2 \cdot A_c}{\omega_0^2} \quad \text{and}$$

$$\frac{dM}{dy_e} = \frac{dM}{d\omega_1} \cdot \frac{d\omega_1}{dy_e} = \frac{\mu_0 \cdot N^2 \cdot A_c}{\omega_1^2}$$

If $|\omega_0| = |\omega_1|$

$$f_e = i_1 \cdot i_2 \cdot \left[\frac{2 \cdot \mu_0 \cdot N^2 \cdot A_c}{\omega_0^2} \right] = K_e i_1 i_2, \quad (25)$$

for a constant d.c. i_1

$$\text{where } K_e = \left[\frac{2 \cdot \mu_0 \cdot N^2 \cdot A_c}{\omega_0^2} \right]$$

IN Laplace domain

$$\frac{F_e(s)}{I_2(s)} = K_e \quad (26)$$

Throughout the derivation it has been assumed that magnetization is uniform and linear to current. But this is not true for low as well as high current region (due to saturation). With certain modification, such as supplying a d.c. bias to the a.c. magnet the operating point may be raised to a linear part [see appendix-B]. With this modification the analysis changes very little, only a static term will be added to force equation.

Thus, the biasing current being I_4 ,

$$f_e = i_1 \cdot i_2 \cdot \left[\frac{2 \cdot \mu_0 \cdot N^2 \cdot A_c}{\omega_0^2} \right] + i_1 \cdot i_4 \cdot \left[\frac{2 \cdot \mu_0 \cdot N^2 \cdot A_c}{\omega_0^2} \right] \quad (27)$$

But as far as dynamics is concerned the static part may be kept aside. The another advantage of using the d.c bias is to provide a static force against thrust force during cutting, thereby the static deflection will be minimized. But this deflection is not controlled actively as for each cutting condition the amount of d.c bias is to be changed. Thus, equation (26) is valid only for dynamic conditions.

Due to the inductive load of magnet at the output of the power amplifier circuit the current i_2 will change with frequency for a definite output voltage at amplifier terminal.

The transfer function $I_2(s)/V(s)$ can be determined in the following way.

The magnetic coil is a parallel combination of inductor (L_{22}) and a resistance (R). From the Fig. [2.4] we get

$$L_{22} \frac{di_a}{dt} = v = R \cdot i_b$$

In Laplace domain the equations become

$$V(s) = L_{22}s \cdot I_a(s)$$

$$\text{and } V(s) = R \cdot I_b(s)$$

$$\text{then } I_2(s) = I_a(s) + I_b(s) = V(s) \cdot \left[\frac{1}{L_{22}s} + \frac{1}{R} \right] \quad (28)$$

$$\text{Thus } \frac{F_e(s)}{V(s)} = G_e(s) = K_e \cdot \left[\frac{1}{L_{22}s} + \frac{1}{R} \right] \quad (29)$$

2.3 ACCELERATION FEED-BACK CONTROL: MODEL-3

Apart from using relative displacement as measured variable ,the acceleration may also be sensed without any technological limitations. The present model deals with the control system where acceleration has been taken to be the state variable .This modeling has been done for the purpose of the revealing the merits and demerits of this scheme compared to other control schemes such as systems using relative displacement or force as state variable. The only difficulty that may arise is that acceleration signal does not contain any information about long term static deflection. As a result the control system will not be able to handle the static deflection actively .But, as it has been discussed, the d.c bias in the a.c magnet may take care of the static deflection ,at least passively. An accelerometre may be used to sense acceleration at the tip of the bar ie at the cutting edge.

The complete block diagram of the proposed control scheme has been shown in the Fig[2.5]

2.4 FORCE FEED-BACK CONTROL :MODEL-4

In this model cutting force has been taken to be the quantity to be measured. Sensing of the force has certain advantages than the sensing of relative displacement or acceleration. Firstly, force carries the static as well as dynamic information and secondly placing of the force transducer in the hole is not a difficult job.

Fig.[2.6] shows the complete block diagram of the above mentioned control system.

2.5 SIMULATION STUDIES OF THE PROPOSED MODELS

The main objectives of any chatter-control-system is to stabilize the cutting process and its interaction with the elastic system of the machine-fixture-tool-workpiece system. The models of the control system, described so far must be capable of tackling the instability of the uncontrolled system (MODEL-1). For simulating the models proper values of the parameters ,such as K_c, K_d etc., are needed ,which are not readily available and require lengthy experimentations. But some representative values (used in literature) will judge the properties of the systems very effectively. For a comparative studies of the models the following values have been used.

1. A 45 cm. long side cut boring bar of $3 \times 4 \text{ cm}^2$ cross-section has been selected .

The natural frequency of the bar for its fundamental mode of vibration can be calculated by the formula

$$\omega_1 = \frac{a^2 \cdot \lambda_1}{l^4} ,$$

where $\lambda_1 = 1.875$,as has been discussed earlier.

2. System damping $\xi_1 = 0.08$,determined experimentally.

3. Cutting stiffness $K_c = 100 \text{ kg/cm}$. (ASSUMED)

4. penetration coefficient K_d is nothing but a stabilization factor ,built in the cutting process itself. It's value can be represented by the formula

$$K_d = \frac{C_p \cdot K_c}{N_0}$$

where $C_p = .117$ (mostly used in the literature)

N_0 = rpm of the spindle of the machine = 500

5. resistance of the magnetic coil $R = 3 \Omega$

6. inductance of the coil can be calculated by the formula

$$L_{22} = \frac{A_c N^2 \mu_r}{l_c} \cdot 10^{-9} \text{ Henry}$$

where A_c = area of the core = $3 \times 4 \text{ cm}^2$

l_c = length of the magnet = 6 cm.

N = no of coils / cm. = 118

μ_r = relative permeability of magnetic material = 1500

7. d.c current in the magnetic coil $i_1 = 2.5 \text{ amp.}$

8. magnetic permeability $\mu_0 = 10^{-7} \text{ weber/amp.m}$

9. gap between the magnets $w_0 = 0.5 \text{ cm}$

10. overlap factor $\mu = 1$

11. elastic modulus of boring bar material = $2 \times 10^6 \text{ kg/cm.}$

12. specific mass of boring bar material $\gamma = 0.0078 \text{ kg/cm}^3$.

2.5a STABILITY CRITERION :

The conventional way of ensuring stability is to raise the minimum real part of the dynamic compliance of the machine tool above -0.5 ,for full regenerative chatter ($\mu = 1$).Though this stability criterion can predict absolute stability ,but it is incapable of

forecasting the relative stability. This shortcoming can be overcome by newer technique of analysing stability [12]. Regeneration spectrum theory is strongly able to ensure the absolute as well as relative stability of the system [appendix-C].

If $P(s) - Q(s).e^{-sT} = 0$, be form of characteristics equation of the system and α_0 be the real part of the least stable root of that equation, then in the frequency (ω) domain the following relation can be written

$$|R(\alpha_0 + j\omega)| = \frac{|Q(\alpha_0 + j\omega)|}{|P(\alpha_0 + j\omega)|}$$

Now if $|R_{\max}(\alpha_0 + j\omega)| < 1$, the system is stable absolutely and magnitude of R_{\max} will be the indicative value of the relative stability. Thus the system giving $|R_{\max}(\alpha_0 + j\omega)| = 0.5$ will be more stable than, for example, $|R_{\max}(\alpha_0 + j\omega)| = 0.7$.

Following the above theory the proposed models have been analysed.

2.5b SIMULATION OF MODEL-1

Overall transfer function of the uncontrolled system is

$$T_1(s) = \frac{G_t(s)}{1 + G_t(s) [K_c(1 - \mu.e^{-T.s}) + K_d.s]} \quad (30)$$

Characteristics equation is

$$1 + G_t(s).K_c.(1 - \mu.e^{-T.s}) + G_t(s).K_d.s = 0 \quad (31)$$

Then,

$$R(s) = \frac{\mu \cdot K_c \cdot G_t(s)}{1 + G_t(s) \cdot K_c + G_t(s) \cdot K_d \cdot s} \quad (32)$$

In the frequency domain putting $s = \alpha_0 + j \cdot \omega$, we get

$$|R(\alpha_0 + j \cdot \omega)| = \frac{\mu \cdot K_c \cdot |G_t(\alpha_0 + j \cdot \omega)|}{|1 + G_t(\alpha_0 + j \cdot \omega) [K_c + K_d \cdot (\alpha_0 + j \cdot \omega)]|} \quad (33)$$

A plot of $|R(\alpha_0 + j \cdot \omega)|$ vs. ω is the regeneration spectrum of the system for the assumed values of the system parameters. this is shown in Fig. [2.7] .

2.5c SIMULATION OF MODEL-2

Closed loop transfer function of the displacement feed-back system is

$$T_2(s) = \frac{G_t(s)}{1 + G_t(s) [K_c(1 - \mu \cdot e^{-T \cdot s}) + K_d \cdot s] + G_e(s) G_{et}(s) \cdot K} \quad (34)$$

$$R_2(s) = \frac{\mu \cdot K_c \cdot G_t(s)}{1 + G_t(s) \cdot K_c + G_t(s) \cdot K_d \cdot s + G_e(s) G_{et}(s) \cdot K} \quad (35)$$

$$|R_2(\alpha_0 + j \cdot \omega)| = \frac{|A(\alpha_0 + j \cdot \omega)|}{|B(\alpha_0 + j \cdot \omega)|} \quad (36)$$

where

$$A(\alpha_0 + j \cdot \omega) = \mu \cdot K_c \cdot G_t(\alpha_0 + j \cdot \omega) \quad (37)$$

and

$$B(\alpha_0 + j.\omega) = 1 + G_t(\alpha_0 + j.\omega) \left[K_c + K_d.(\alpha_0 + j.\omega) \right] + K.G_{et}(\alpha_0 + j.\omega).G_e(\alpha_0 + j.\omega) \quad (38)$$

Fig.[2.8] shows the corresponding regeneration spectrum ,for the value of gain $K= 0.1$

2.5d SIMULATION OF MODEL-3

Closed loop transfer function of the acceleration feed-back system is as follows:

$$T_3(s) = \frac{G_t(s)}{1 + G_t(s) \left[K_c(1 - \mu.e^{-T.s}) + K_d.s \right] + s^2 G_e(s) G_{et}(s).K} \quad (39)$$

and

$$R_3(s) = \frac{\mu.K_c.G_t(s)}{1 + G_t(s).K_c + G_t.K_d.s + s^2 G_e(s) G_{et}(s).K} \quad (40)$$

In frequency domain

$$|R(\alpha_0 + j.\omega)| = \frac{|A(\alpha_0 + j.\omega)|}{|B'(\alpha_0 + j.\omega)|} \quad (41)$$

where

$$B'(\alpha_0 + j.\omega) = 1 + G_t(\alpha_0 + j.\omega) \left[K_c + K_d.(\alpha_0 + j.\omega) \right] + (\alpha_0 + j.\omega)^2.K.G_{et}(\alpha_0 + j.\omega).G_e(\alpha_0 + j.\omega) \quad (42)$$

Corresponding regeneration spectrum is shown in fig.[2.9] ,

for $K = 0.1$

2.5e SIMULATION OF MODEL-4

Closed loop transfer function of the control system with force as a state variable is

$$T(s) = \frac{G_f(s)}{1 + G_f(s) [K_c(1 - \mu \cdot e^{-T \cdot s}) + K_d \cdot s]} \quad (42)$$

where

$$G_f(s) = G_t(s) - K \cdot G_{et}(s) \cdot G_e(s) \quad (43)$$

$$R_4(s) = \frac{K_c \cdot G_f(s) \cdot \mu}{1 + K_c \cdot G_f + K_d \cdot G_f \cdot s} \quad (44)$$

In the frequency domain we have

$$|R_4(\alpha_0 + j \cdot \omega)| = \frac{K_c \cdot \mu \cdot |G_f(\alpha_0 + j \cdot \omega)|}{|1 + K_c \cdot G_f(\alpha_0 + j \cdot \omega) + K_d \cdot G_f(\alpha_0 + j \cdot \omega) \cdot (\alpha_0 + j \cdot \omega)|} \quad (45)$$

The corresponding regeneration spectrum has been shown in Fig.[2.10].

2.6 RESULTS AND DISCUSSION : COMPARISON OF MODELS

It is clear from the theoretical regeneration spectrum for the above four models that it is possible to stabilize the unstable cutting process and elastic system interaction ,with the help of proposed control scheme. All three types of control actions are capable of tackling the instability after a certain value of amplifier gain. But due to the difference in the response of those control systems to gain ,all are not equally competent in practical environment. Acceleration feed-back system can show good stability condition at very low value of gain (K) (fig.[2.11]) while displacement feed-back system requires very high amplifier gain for stability (Fig.[2.12]). Force monitoring scheme is also dependent on high value of gain for stability. Furthermore, the displacement feed-back and force feed-back system show (Fig.[2.13]) an abrupt worsening of stability up to a certain value of gain and after a very high value of gain they stabilize. In electrical operation high gain functioning should always be avoided ,because any spurious signal(noise) will be amplified and distort the signal proper. More over the high gain electrical instrument for liner operation may add cost to the system .As acceleration feed-back system becomes stable at very low value of amplifier gain it can be preferred to the other schemes ,despite of its incapability of reducing high order static deflection. But in this scheme the static deflection can also be controlled .This discussion has been made in detail in the section 4.3.

The theoretical stability chart for uncontrolled and acceleration feed-back systems has been shown in the

Fig.[2.14].The figure reveals the improvement in the stability limit in speed domain.The figure does not reveal the true picture of what is happening practically ,as the dependence of K_c on the cutting speed has not been taken into account.But the objective of showing the improvement in the stability is fulfilled.

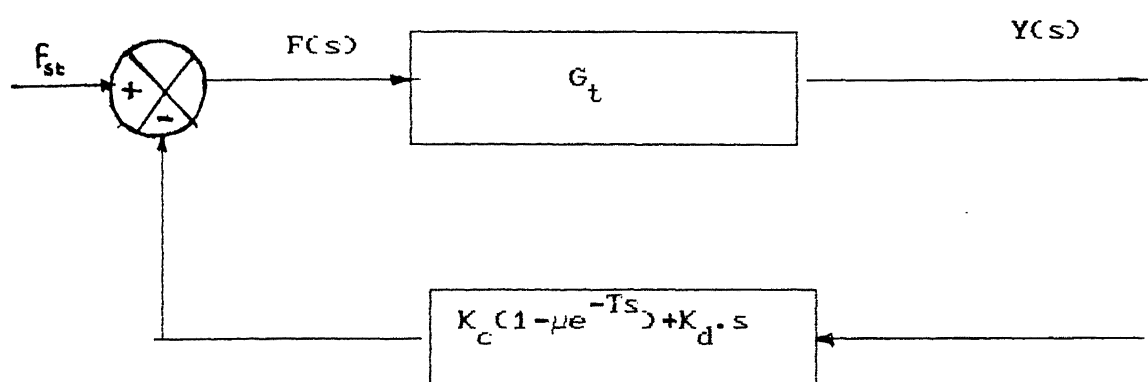


Fig. 2.1 BLOCK DIAGRAM OF UNCONTROLLED SYSTEM (MODEL - 1)

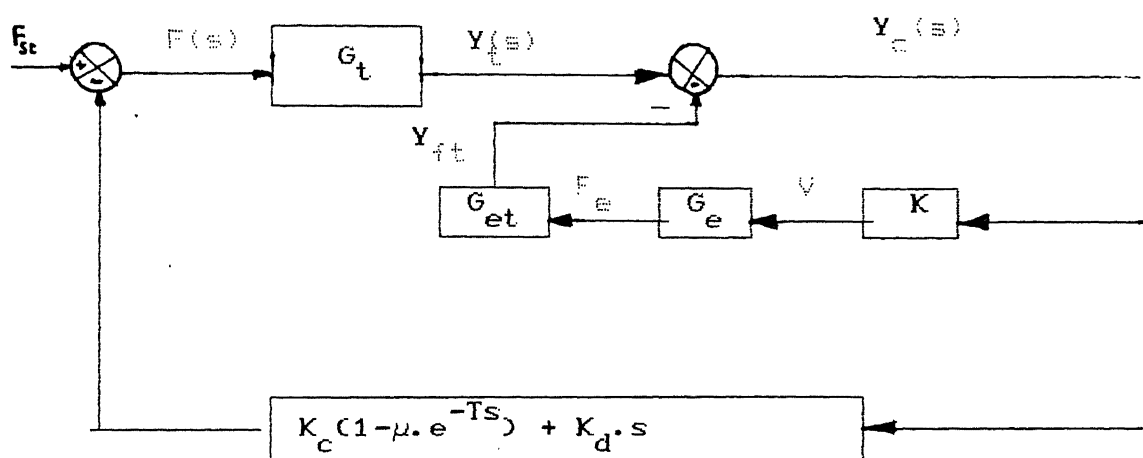


Fig.2.2 BLOCK DIAGRAM OF DISPLACEMENT FEED-BACK CONTROL SYSTEM (MODEL-2)

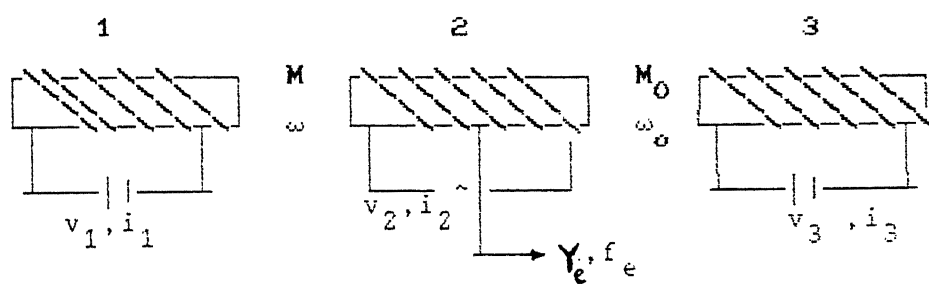


fig. 2.3 ARRANGEMENTS OF MAGNETS
IN THE EXCITER

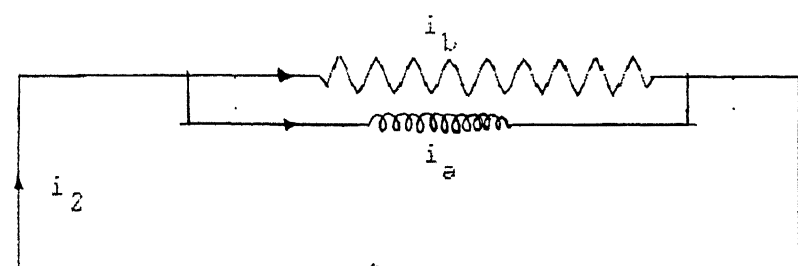


fig. 2.4 EQUIVALENT CIRCUIT DIAGRAM
OF THE MAGNETIC COIL

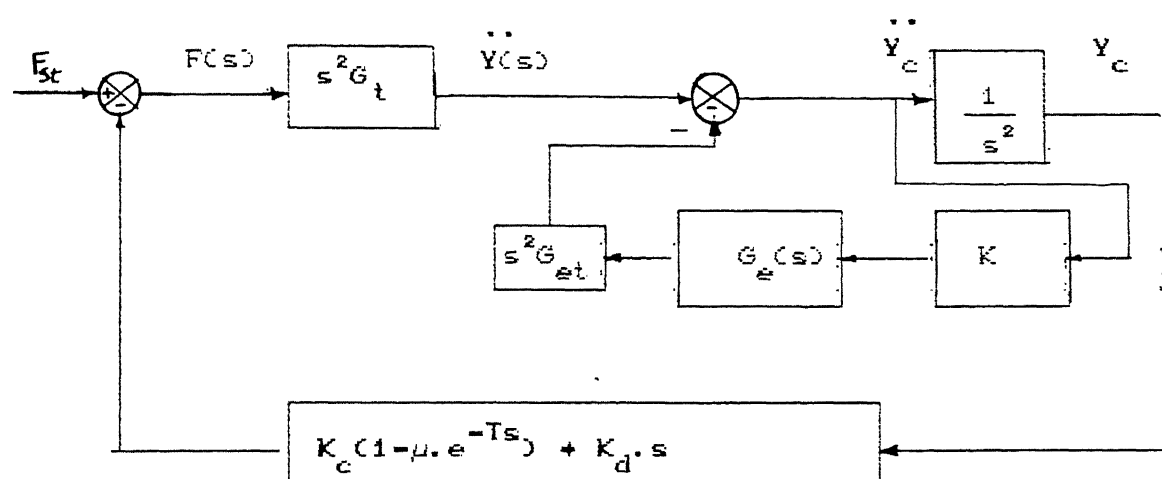


Fig. 2.5 BLOCK DIAGRAM OF ACCELERATION FEED-BACK CONTROL SYSTEM (MODEL-3)

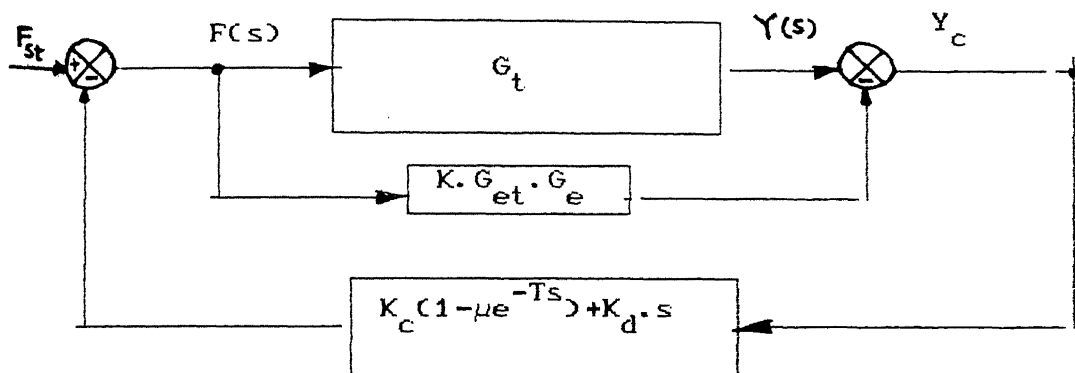


Fig.2.6 BLOCK DIAGRAM OF FORCE FEED-BACK SYSTEM (MODEL-4)

Fig. 2.7 REGENERATION SPECTRUM 1

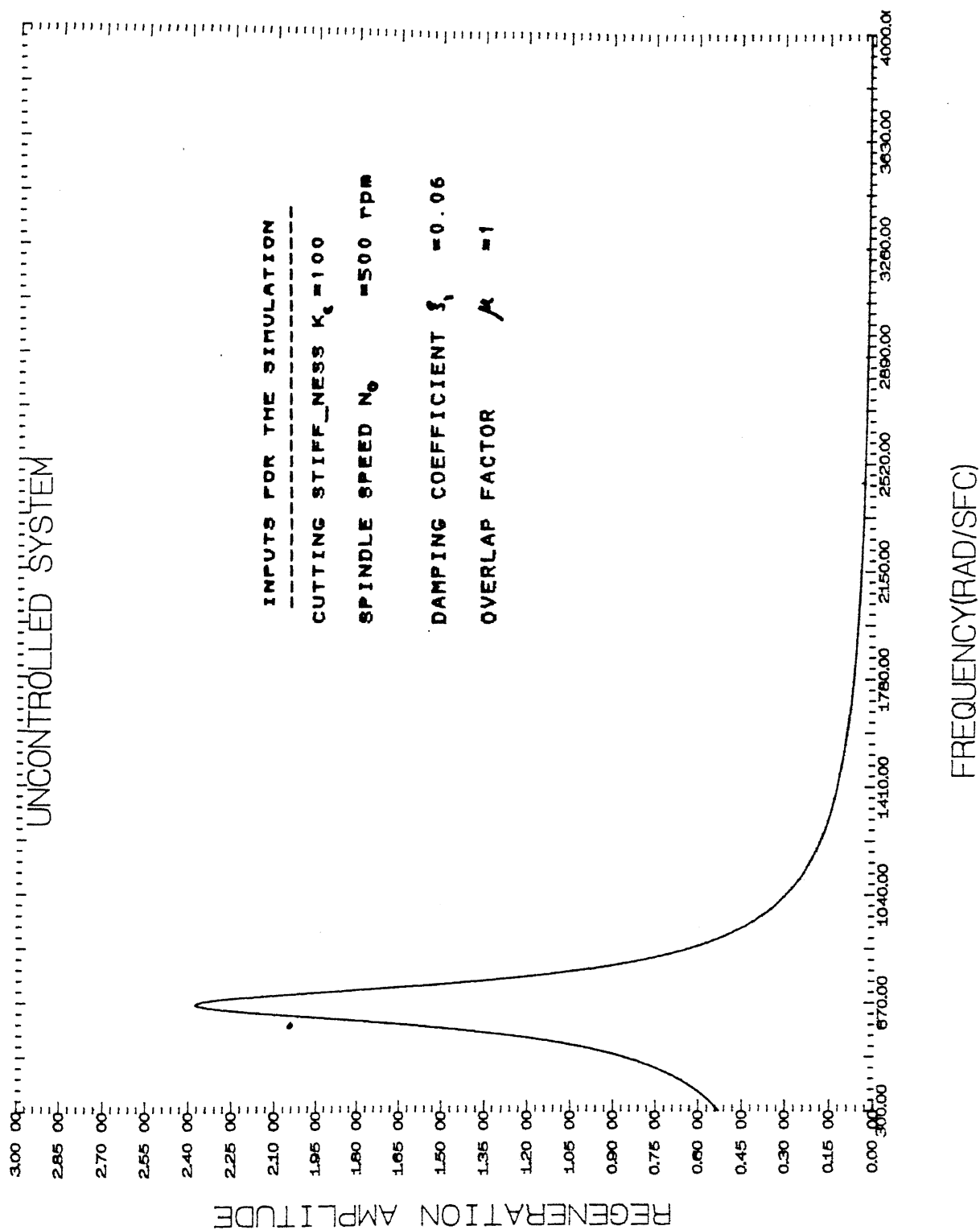


Fig. 2.8 REGENERATION SPECTRUM 2

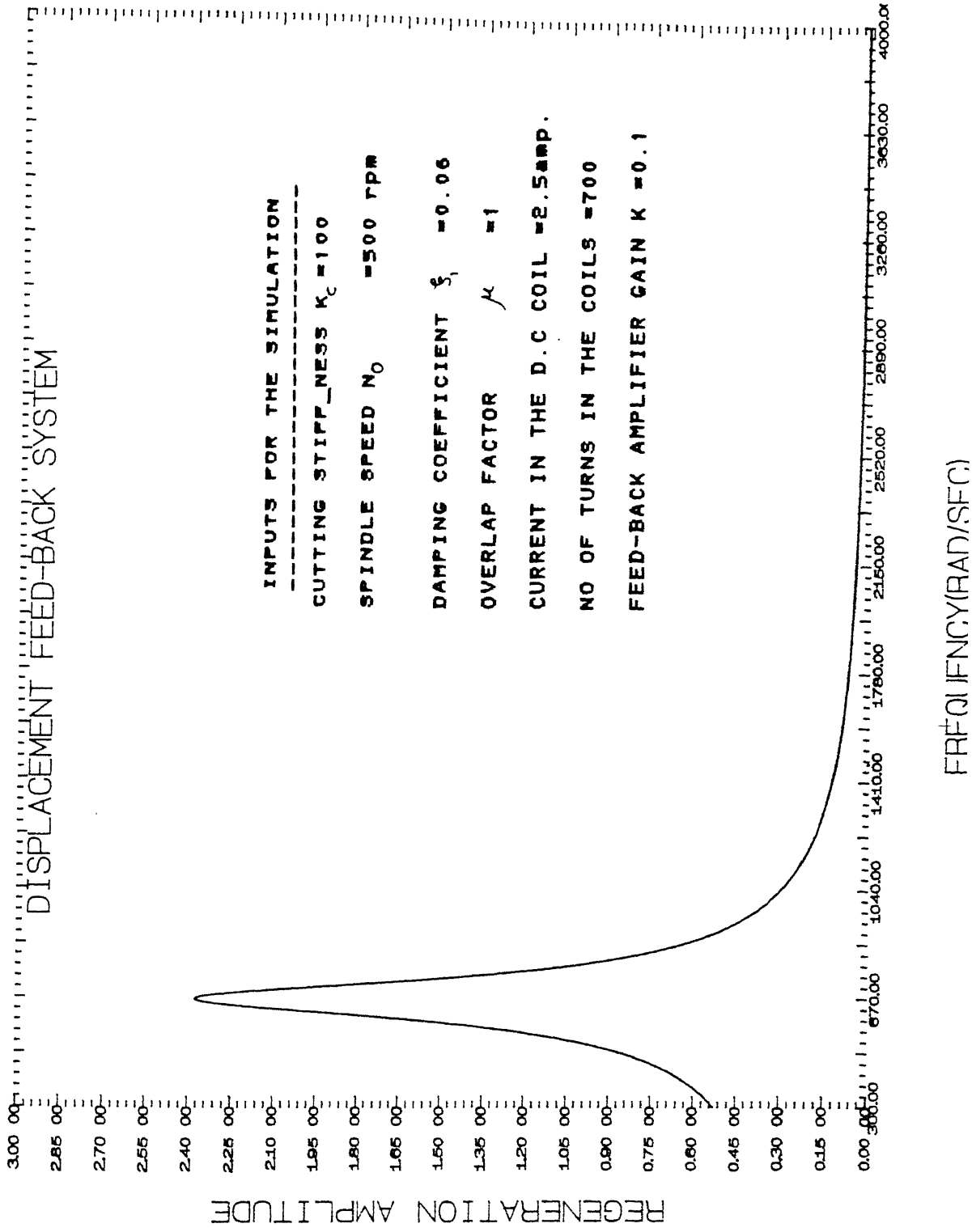


fig. 2.9 REGENERATION SPECTRUM 3

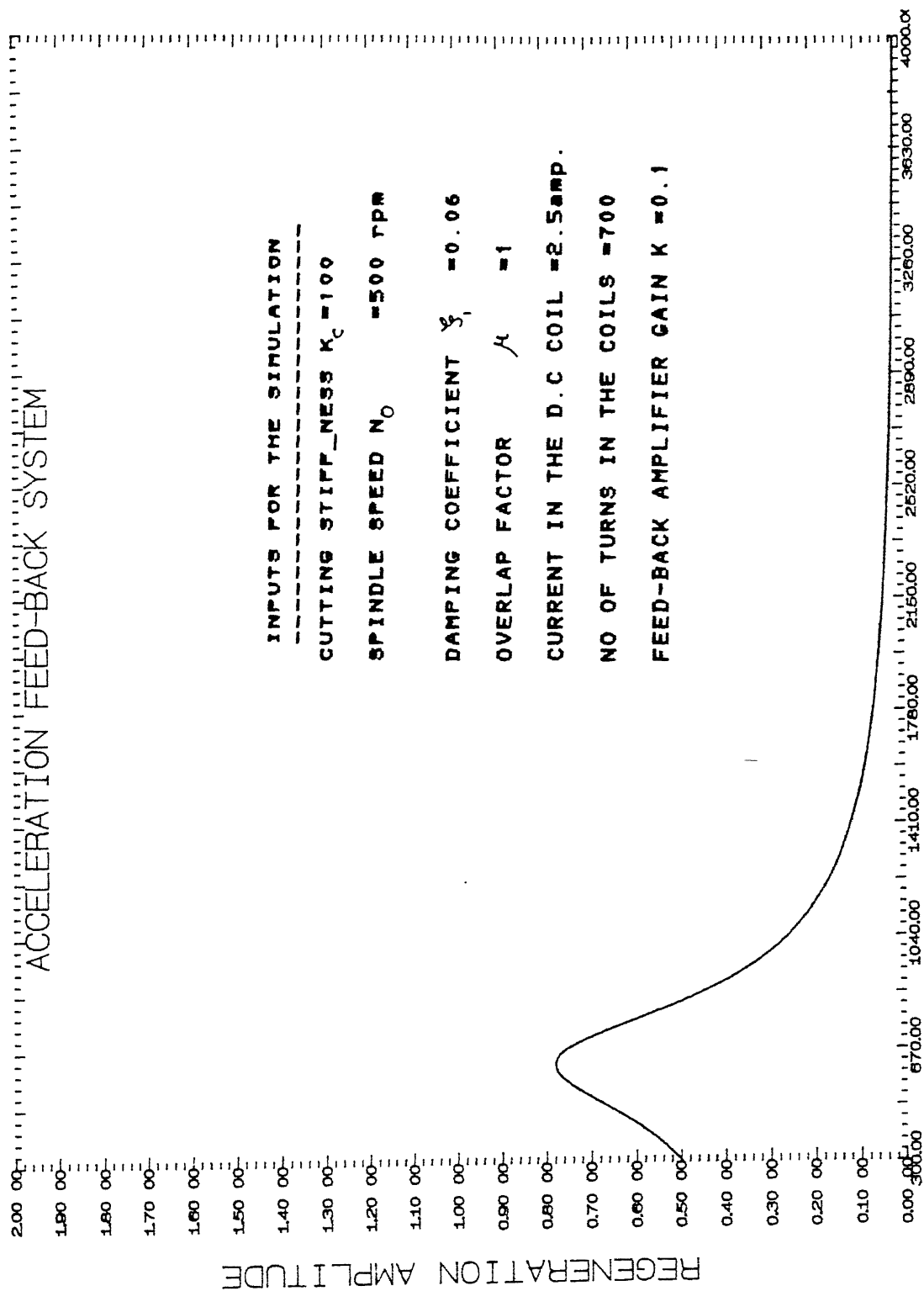


Fig. 2.10 REGENERATION SPECTRUM 4

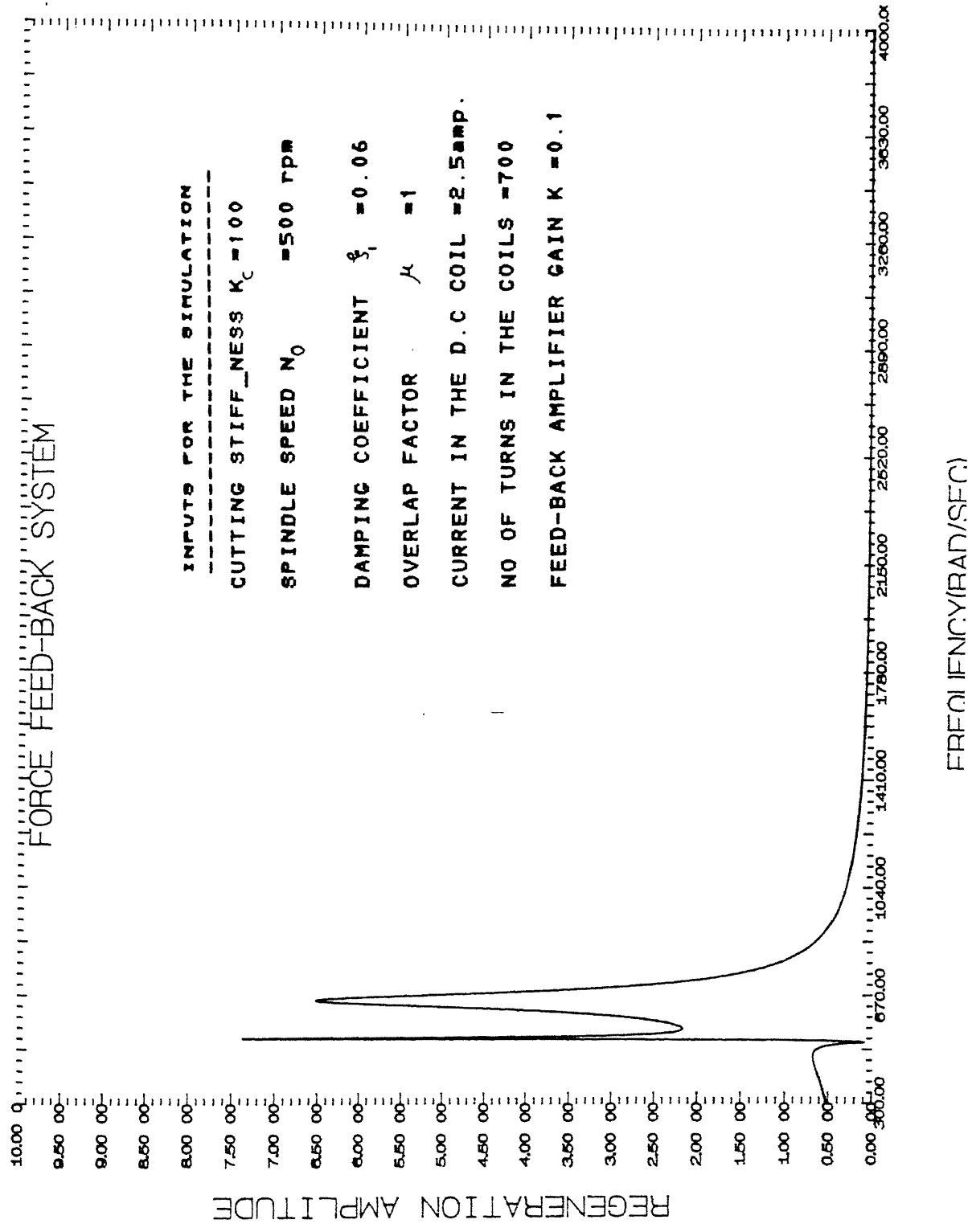


Fig. 2.11 ACCELERATION FEED-BACK SYSTEM

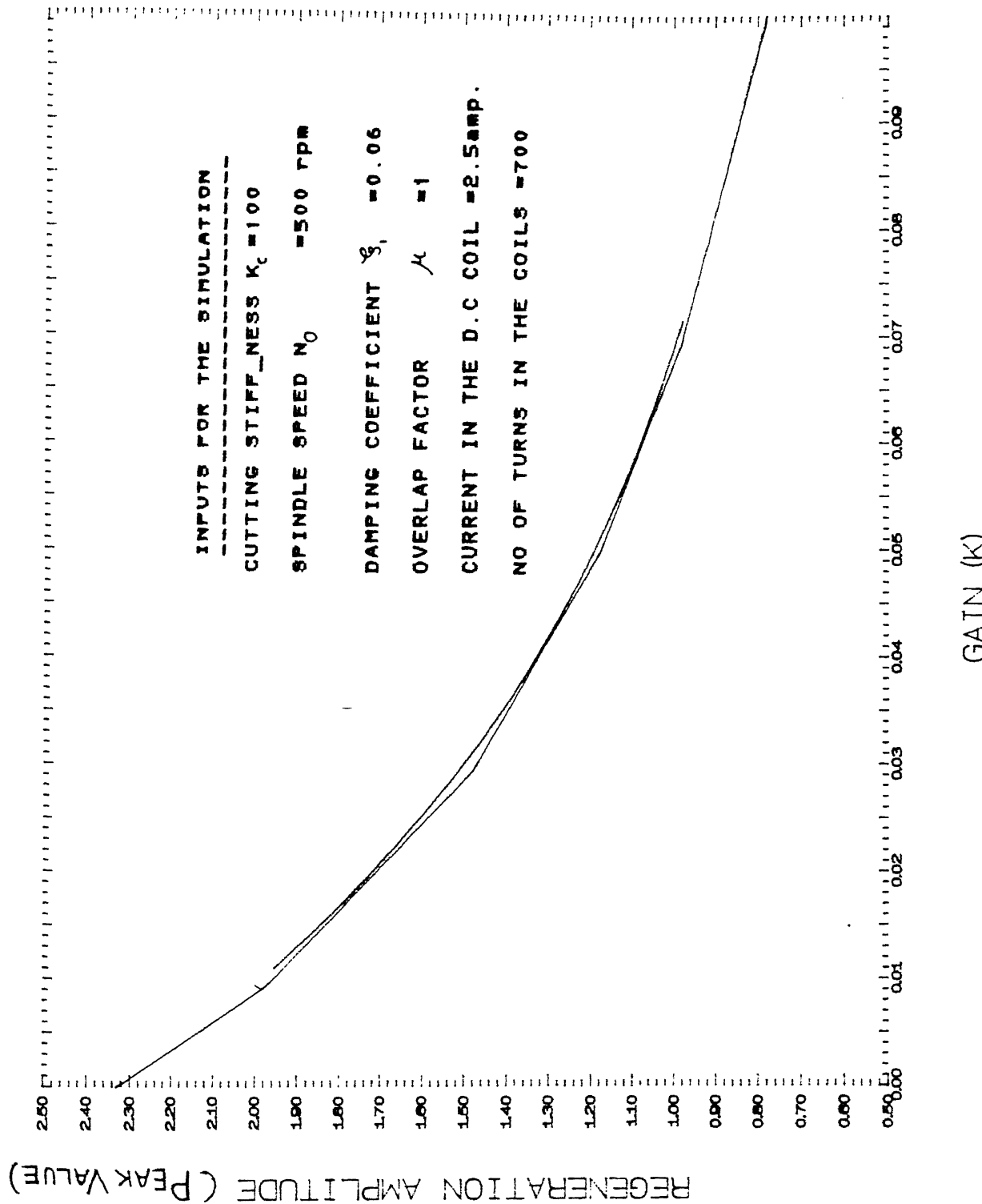


Fig. 2.12 DISPLACEMENT FEED_BACK SYSTEM

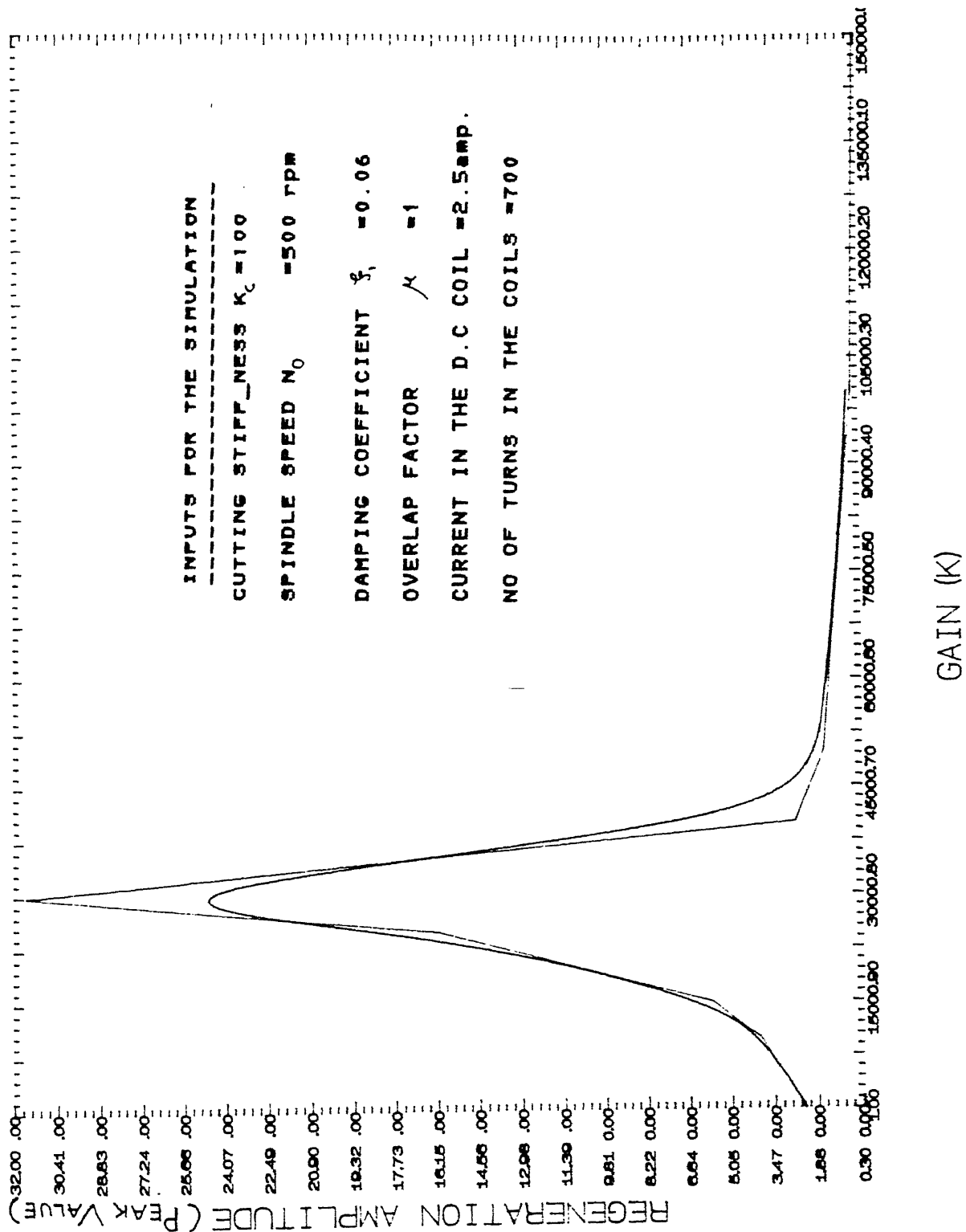


Fig. 2.13 FORCE FEED-BACK SYSTEM

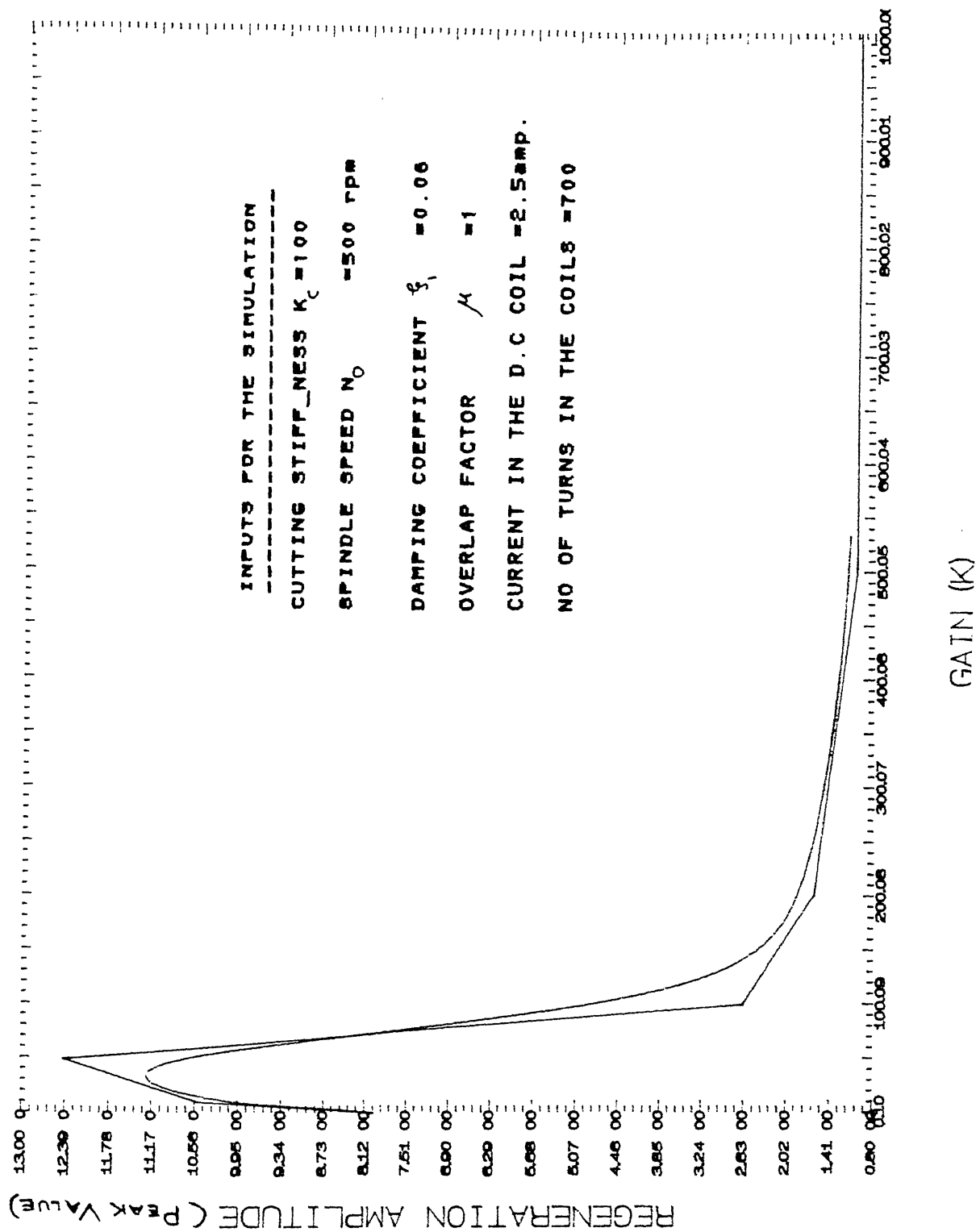
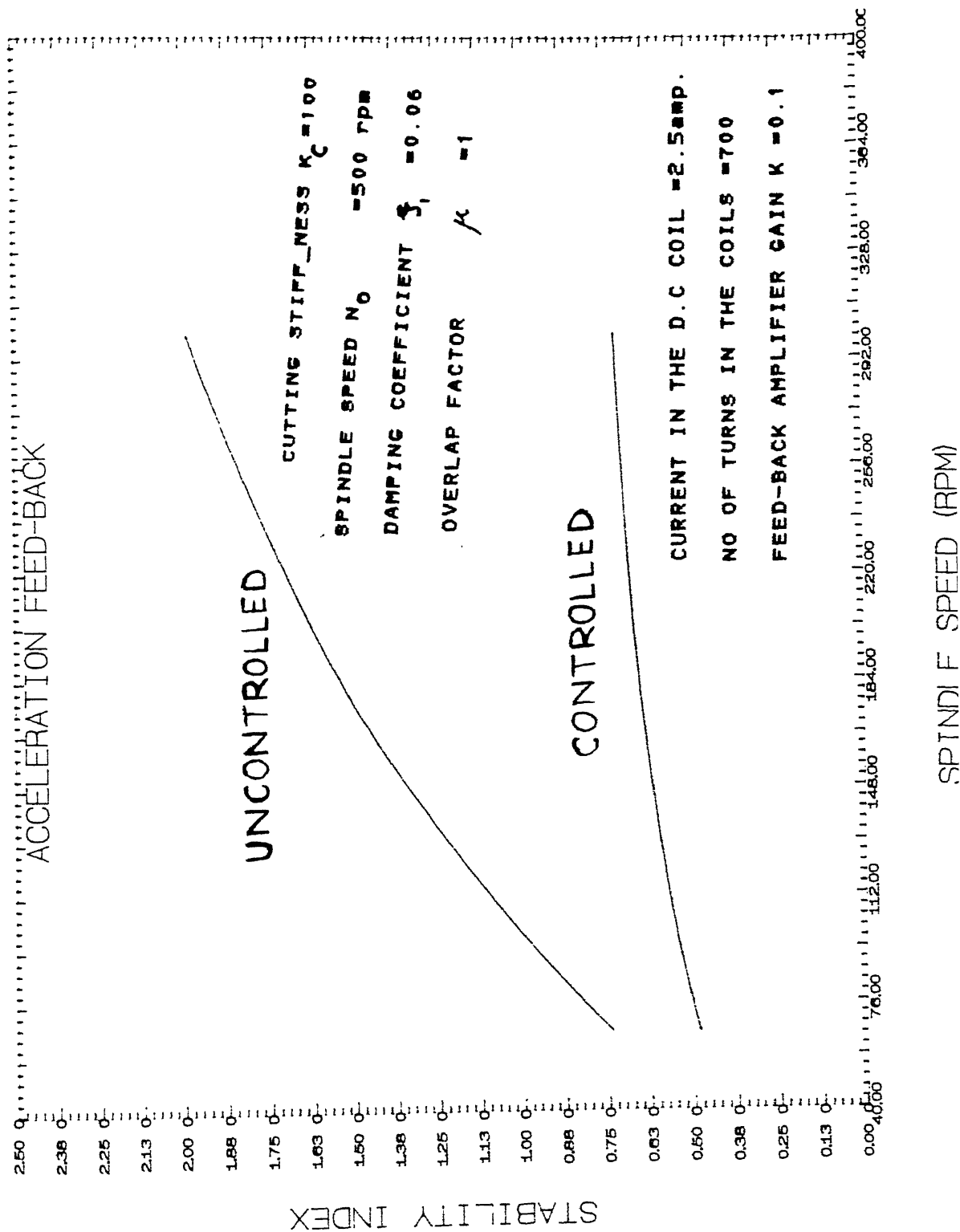


Fig. 2.14 STABILITY CHART



CHAPTER-III

DESIGN AND CALIBRATION OF THE EXPERIMENTAL SET UP

In chapter-ii a comparative study of acceleration ,displacement and force feed-back systems has been made.The investigation revealed that acceleration feed-back system is highly stabilized at very low value of feed-back path gain compared to displacement and force feed-back control system.Due to certain advantages ,as has been discussed earlier , of acceleration feed-back control it has been selected for experimental investigation .

3.1 AN OVERALL DESCRIPTION OF THE EXPERIMENTAL SET UP:

Fig.[3.1] shows a schematic diagram of the whole setup,which consists of an accelerometer for the purpose of monitoring the acceleration,amplifier circuit,and the electromagnetic actuator.A 45 cm. long rod of En-steel with 3 cm dia and two milled flat-faces [fig.3.2] has been used as a boring bar.For the purpose of holding the end of the bar is made tapered and fitted into a tapered hole .Besides, it is held tightly back with help of a nut.As it is discussed earlier ,the bar is set in such a position that two milled faces remain perpendicular to the machine bed (ensuring $\alpha_1 = 0$ [see appendix A]),to avoid mode-coupling effect in chip thickness direction.It is not possible to place the exciter at the tip of the bar, ie at the cutting edge,although it is the best place from theoretical point of view.Because of these technological limitations the exciter is placed very close to the base of the bar;the excitation point is 10 cm away from the fixed

end. The exciter [Fig. 3.3] consists of an electromagnet fixed on the boring bar with a rigid clamp and placed in between two electromagnets of constant polarity. The electromagnets of constant polarity are fixed on a rigid structure to avoid their vibration.

An accelerometer is fixed at the tip of the bar i.e near the cutting edge with the help of a magnetic base. The output of the accelerometer is connected to a signal conditioner (charge amplifier). One of the output signals from the signal conditioner goes to the power amplifier circuit and another goes to a single channel of a Hi-corder recorder. The output of the power amplifier is fed to the electromagnet fixed on the boring-bar. The proper connection has been made to maintain a 180° relative phase between the accelerometer signal and the force in the exciter.

3.2 DESIGN OF THE EXCITER:

When an electromagnet fed with an A.C is placed in line with a permanent magnet or an electromagnet of constant polarity, with either of the two being fixed, the other magnet will start vibrating at frequency of the supplied A.C. The dynamics of the exciter has already been discussed in chapter-ii. Electromagnet of constant polarity (supplied with D.C) is preferred to permanent magnets because it is always possible to increase the strength of magnet by supplying more current in the windings, according to necessity. Fig[3.3] shows the arrangements of the magnets. Two electromagnets of constant polarity are used to exploit the following advantages. Firstly, this arrangement will obviously increase the excitation force and as a result the feed-back gain will also increase. On the other hand the excitation force will

bear a linear relationship with the signal current. If a single D.C magnet would have been used the force equation of the exciter becomes

$$f_e = \frac{1}{2} \left[i_1^2 \cdot \frac{d}{dy_e} (L_{11}) + i_2^2 \cdot \frac{d}{dy_e} (L_{22}) \right] + i_1 i_2 \cdot \frac{dM}{dy_e}$$

and L_{11} & L_{22} no more remain invariant to y_e . Consequently follows a quadratic relationship with current, leading to nonlinear dynamics of the exciter.

The core of the electromagnets are made of transformer steel laminations. The size of the core is $3 \times 4 \text{ cm}^2 \times 6 \text{ cm}$. For winding 19-gauge Cu wire has been used. Each magnet consists of 700 windings. Besides, the A.C magnet is provided with another 100 windings, for D.C biasing. This biasing becomes necessary for raising the operating point into the linear part of the magnetization curve [see appendix-B].

The gap between the magnets is maintained at 5mm.

3.3 DESIGN CRITERION OF THE EXCITER:

The exciter should be capable of providing enough force to excite the boring bar as well as it must have frequency response range above the probable chatter frequency. The excitation force can be increased (before saturation of the core takes place) either by increasing the number of turns of the magnetic coil or by supplying more current into the coil. The effect of increasing the turn is more, the excitation force being proportional to the square of the number of turns. But an increased current will produce more heat, affecting proper magnetization, as heat is directly

proportional to the square of the current in the coil. By increasing the number of turns the magnet will act as a choke and will filter out the high frequency oscillation. A contradictory effect that will come into picture is that, larger number of turns will increase the inductance of the coil, and that will offset the relative phase of current in the coil and applied signal voltage. If it is assumed that magnetization does not lag behind the current [appendix-B], then also the 180° out of phase between the signal voltage and applied current in the coil is not maintained. As a result the stability condition will deteriorate. So the number of turns should be the design criterion of the exciter. Fig.[3.5] shows the effect of number of turns on the stability. It can be concluded from the above discussion and from the nature of the curve in fig.[3.5] that number of turns should not be too low and very high. This is the basis of selecting the number of turns to be 700 in the present experiment.

3.4 CALIBRATION OF THE EXCITER:

The frequency response pattern of the exciter is determined experimentally. For this purpose, boring bar is excited by passing a sinusoidal signal of definite voltage level (p-p) and varying frequency, to the exciter. A signal generator is used to provide the same signal. The acceleration level (in mv.) is measured at the tip of the bar with help of an accelerometer and digital oscilloscope. Fig [3.6] shows the typical frequency response curve of the exciter.

Similarly voltage response of the exciter is also obtained by varying the input voltage level and keeping the frequency

constant. Fig [3.7] shows the voltage response curve of the exciter for different frequencies.

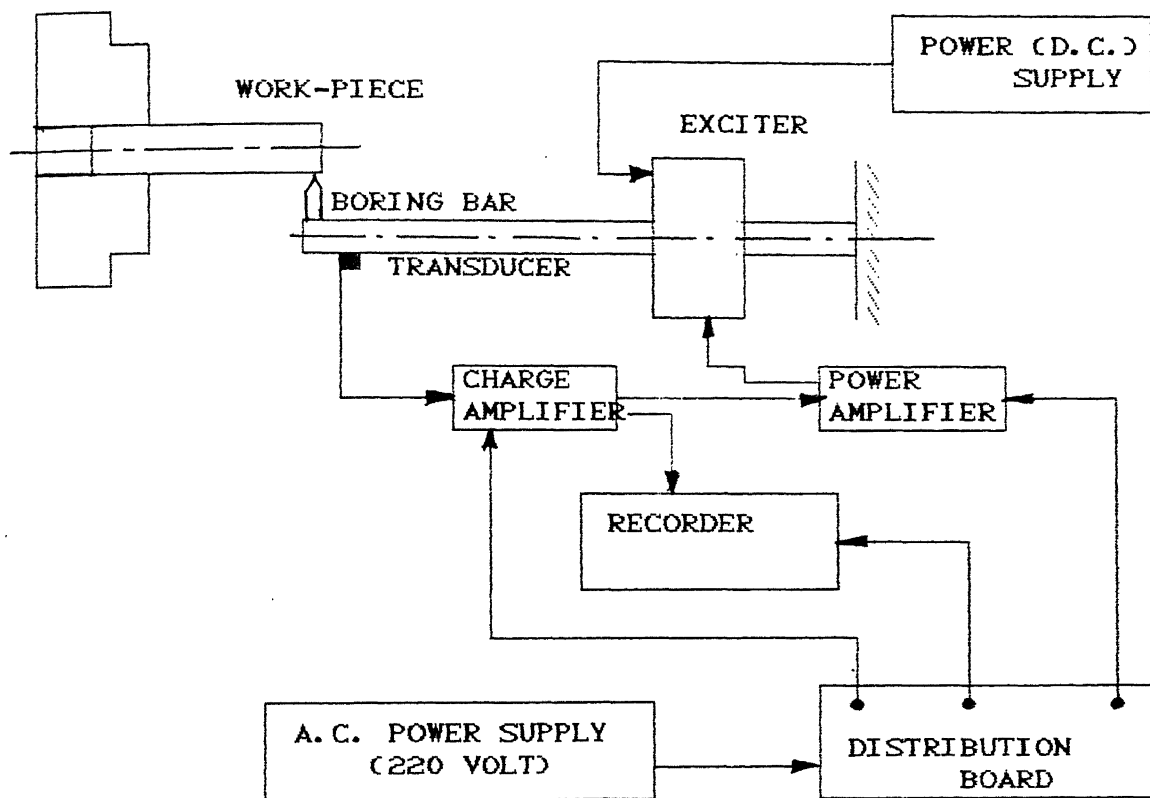


Fig. 3.1 SCHEMATIC DIAGRAM OF THE EXPERIMENTAL SET-UP

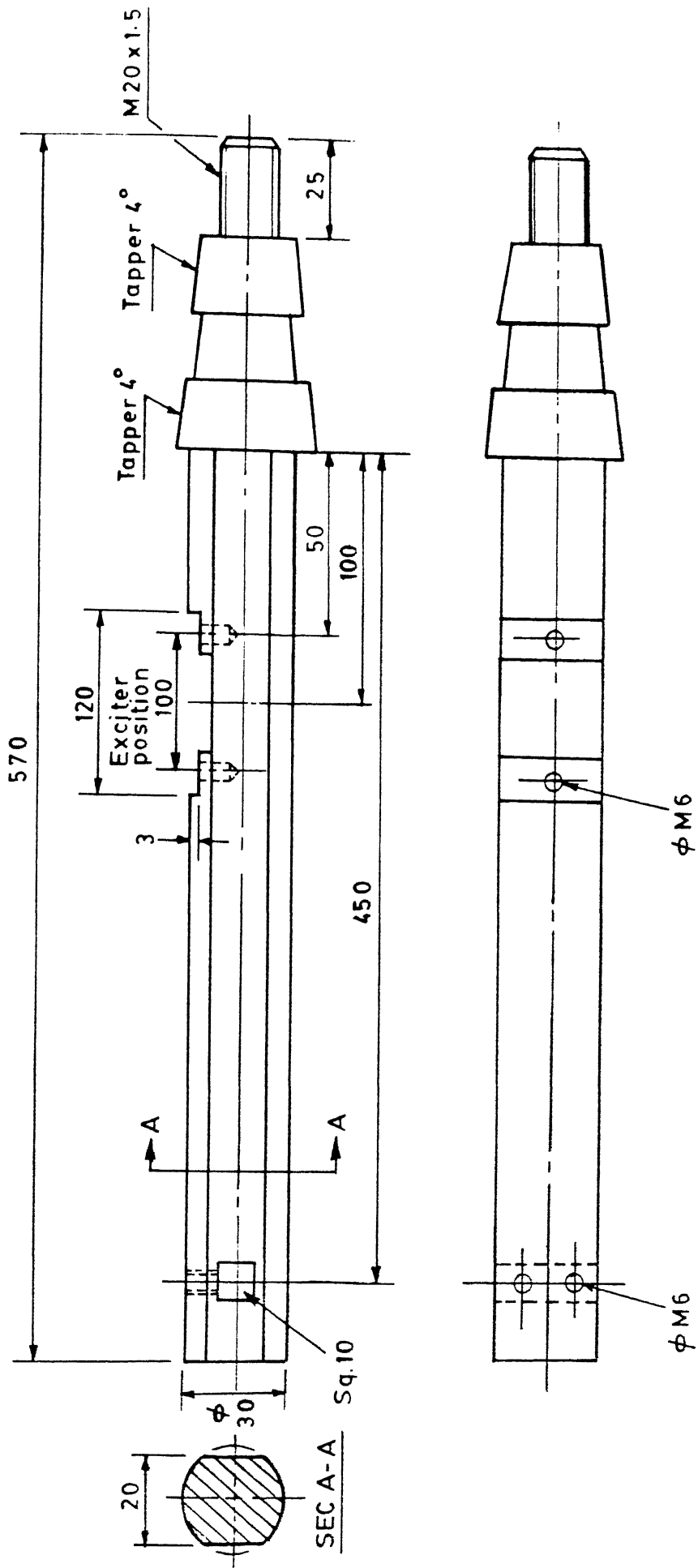


FIG. 3.2 SCHEMATIC DIAGRAM OF THE BORING BAR

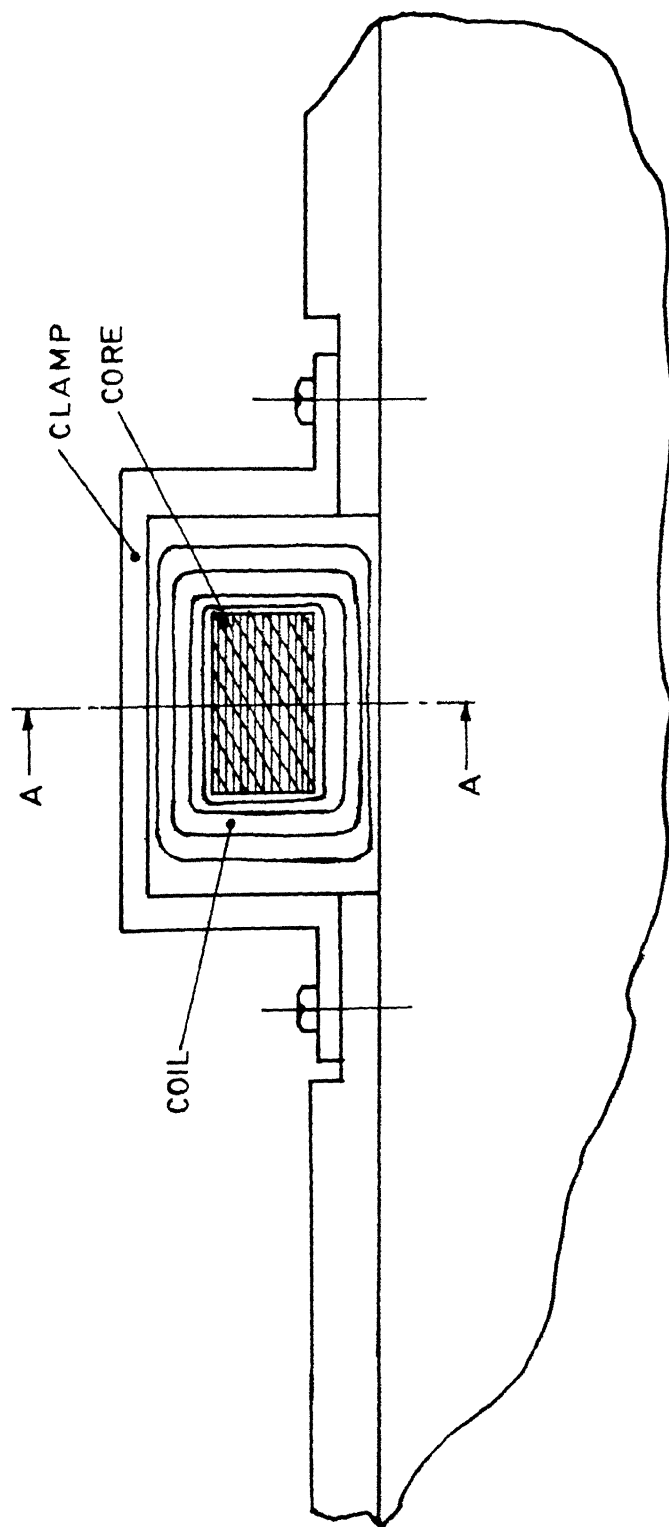


FIG. 3.3 EXPANDED VIEW OF THE EXCITER POSITION AND THE ELECTRO-
MAGNET CLAMPED WITH THE BORING BAR

CENTRAL LIBRARY
Acc. No. **A112177**

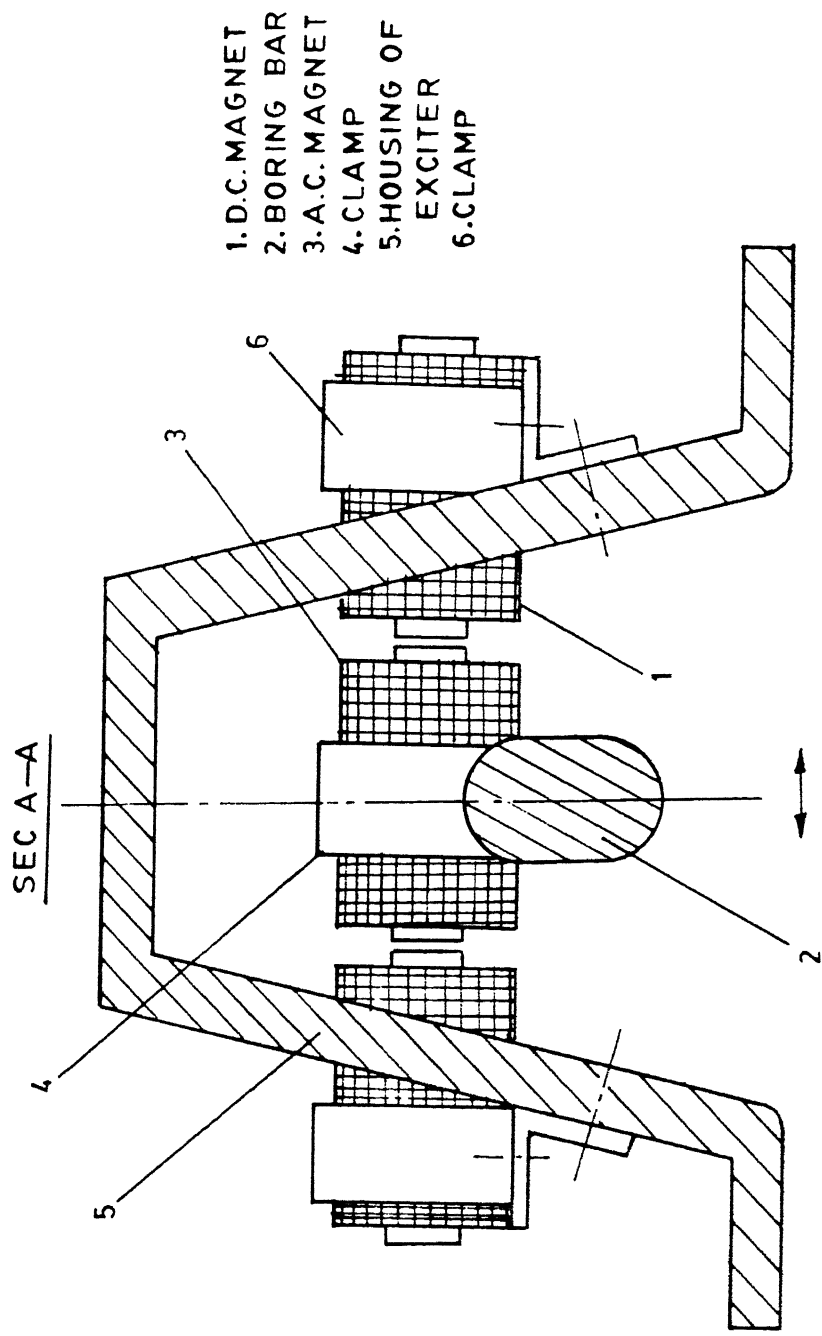
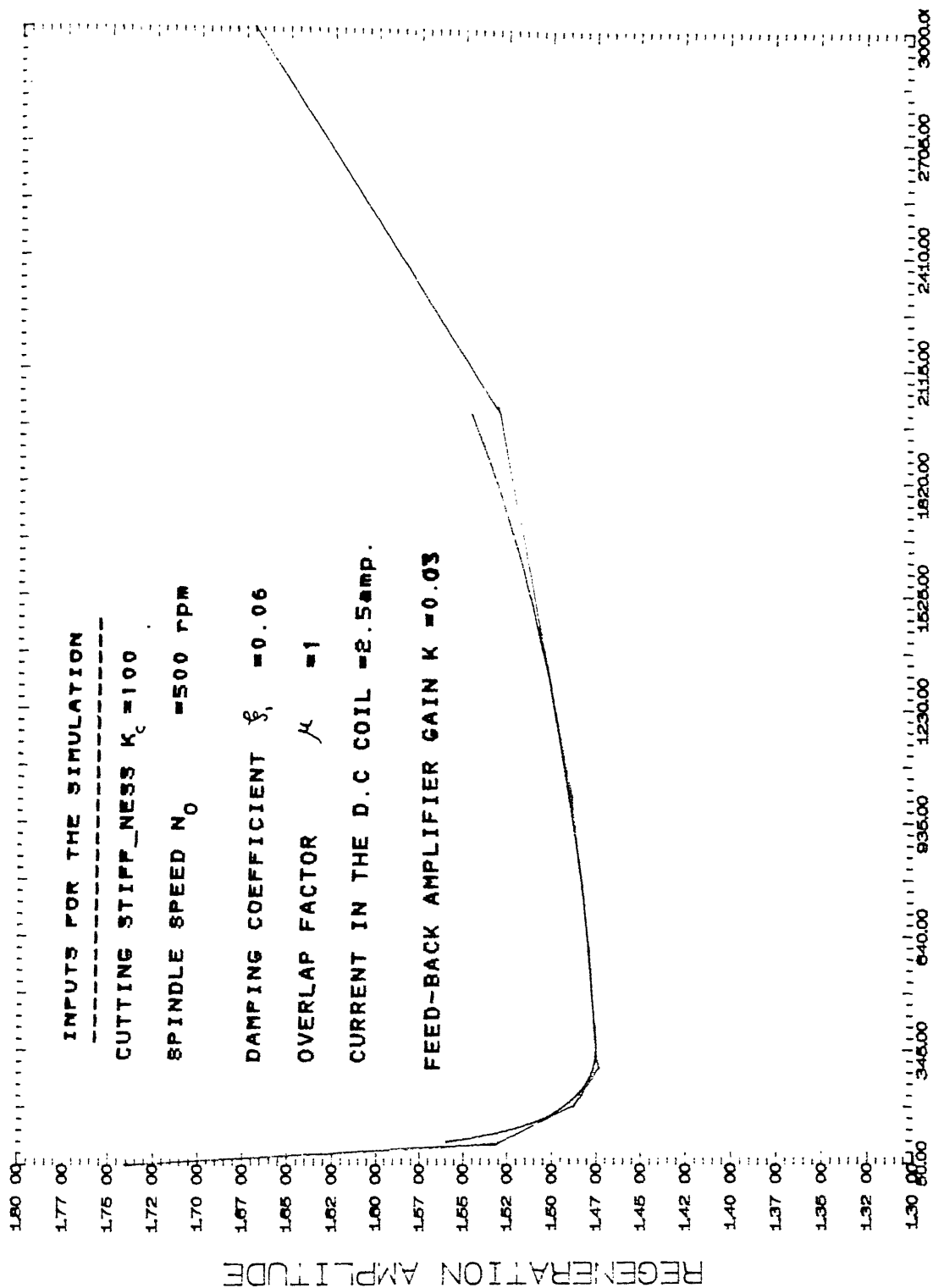


FIG. 3.4 SCHEMATIC DIAGRAM OF EXCITER

Fig. 3.5



NO. OF TURNS

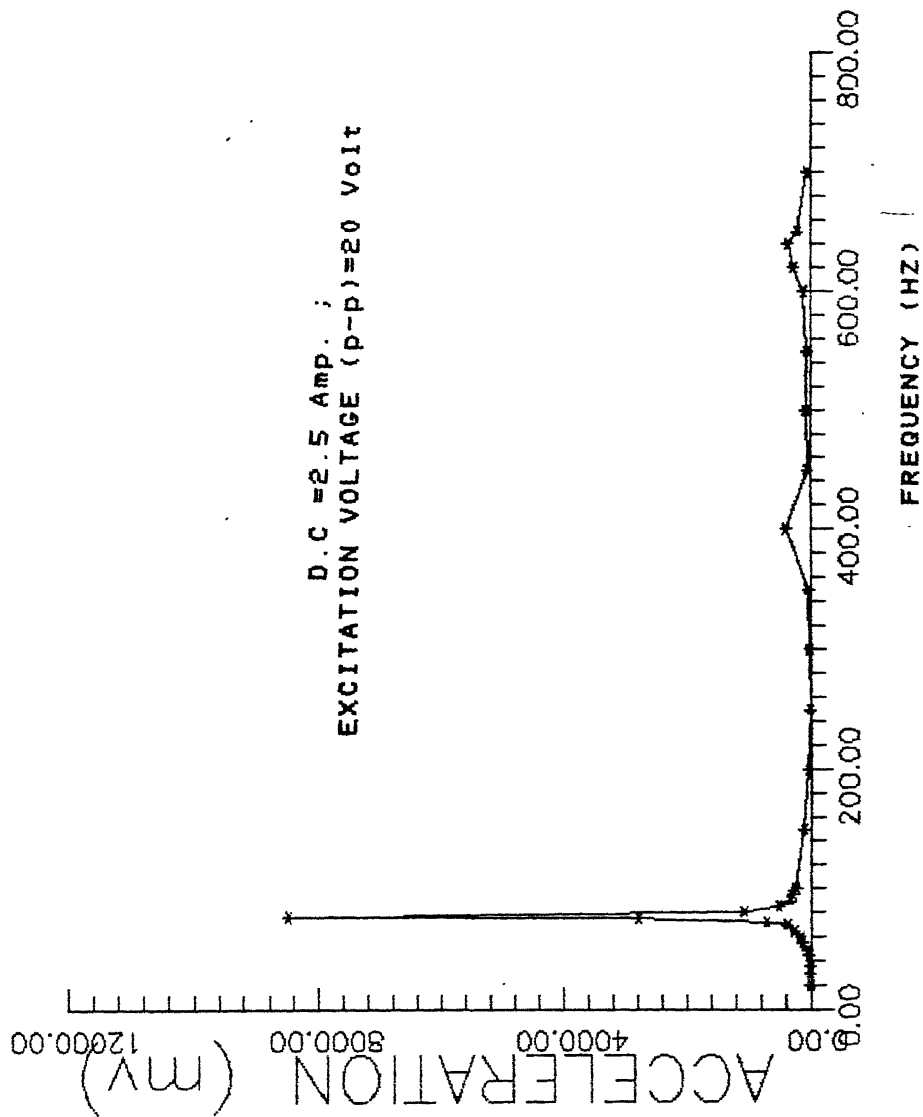
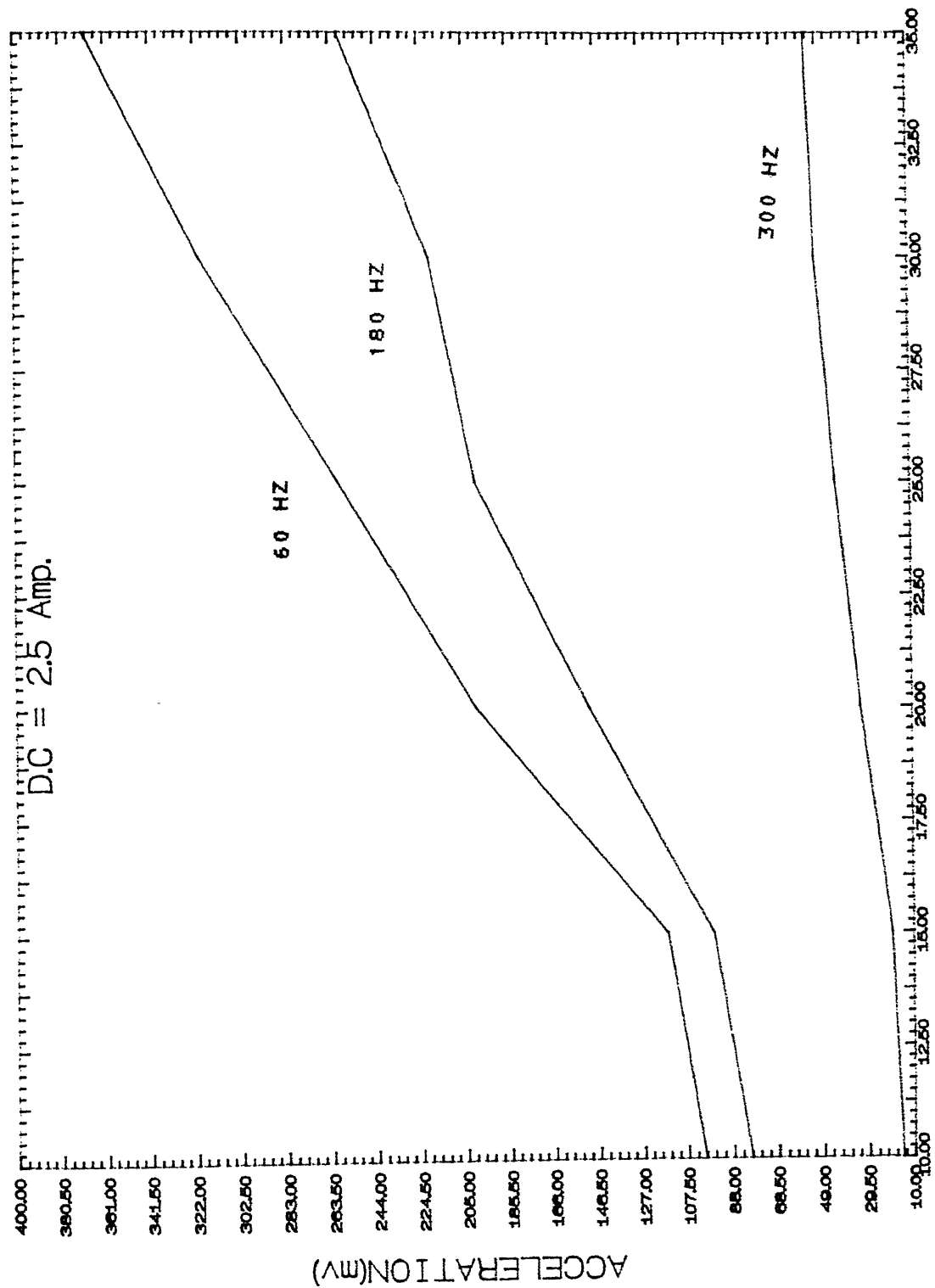


Fig . 3.6. FREQUENCY RESPONSE CURVE OF THE EXCITER

Fig. 3.7 VOLTAGE RESPONSE CURVE OF THE EXCITER



EXCITATION VOLTAGE (p-p)[V]

CHAPTER-IV

EXPERIMENTAL RESULTS AND DISCUSSION

As it has been discussed earlier that regenerative chatter vibration is the most severe type of machine tool vibration ,any chatter control system should be tested for controlling regenerative chatter. Due to its low gain stabilization characteristics ,acceleration feed-back system is convenient to apply practically. In the present experimentation acceleration has been taken to be the controlled variable.

As regenerative chatter condition can conveniently be obtained during grooving ,the proposed control scheme is tested for grooving operation as well as for straight turning, on a lathe. Following cutting conditions are selected for testing:

TABLE-1

R. P. M.	FEED (mm./rev)	WIDTH OF CUT (mm.)	OTHER CONDITIONS
160	0.03	3	workpiece diameter = 20 mm
64	0.046	"	workpiece material. Brass
64	0.092	"	machining operation: grooving
40	0.075	"	rake angle of tool: 30°
40	0.03	"	

TABLE-2

R. P. M	FEED (mm./rev)	DEPTH OF CUT (mm)	OTHER CONDITIONS
320	0.03	0.1	machining operation : orthogonal turning
500	0.03	0.1	

4.1 EXPERIMENTAL PROCEDURE AND RESULTS:

To show the effectiveness of the proposed control technique both controlled and uncontrolled cutting have been done ,for the above said cutting conditions.The experimental results for both controlled and uncontrolled cutting are shown in the Figs.[4.1-4.14].Due to the non-availability of continuous recording instrument,intermittent recording has been done.The recorder has been triggered for 20ms after the interval of 1sec.For each cutting condition 2-5 spectrums are taken in controlled and uncontrolled state.

It is seen from the controlled and uncontrolled vibration pattern that the amplitude of vibration during controlled cutting is less on an average than that of the uncontrolled chatter,for every cutting condition.This obviously reflects the practical feasibility of the proposed control action in reducing chatter level.

4.2 CONCLUSION:

From the vibration pattern it is clear that chatter vibration

contains different frequencies with variable amplitudes. It is also seen that during grooving as time passes the amplitude of vibration increases, which is due to the change in cutting condition. As tool penetrates into the material the cutting velocity continuously reduces, producing higher cutting-stiffness value. It is already established that high cutting-stiffness will result in more instability. Therefore, the vibration in the controlled cutting is also seen to increase with the time, as the experimentation and the theory deals with the constant gain. To control the system with variable cutting condition a time varying gain, depending on the level of vibration should be incorporated with the help of a self-adaptive control scheme.

Because the vibration pattern includes different frequencies of different amplitudes, the magnetic coil of the exciter will carry different level of current for each frequency. Though the frequency with the highest amplitude should be of more interest (as far as regenerative chatter vibration is concerned), any signal of much lower frequency will produce more current and, hence, more excitation in the exciter, giving less priority to the frequency of importance [appendix-D]. Moreover, different signal currents with different frequencies will bear different phase-shifts with the signal voltage. So it is not possible for the exciter to react to all the frequencies equally. After-all it is not easy to predict about the behavior of a magnet being fed by current with different frequencies [Fig. 4.15]. These problems of course, can be avoided with the help of a lock-in amplifier, with which only the frequency with the maximum amplitude can be passed through the exciter. The result in that case would have

been better than the present one. But due to the non-availability of the proper hard-ware, this can't be applied during experimentation.

4.3 SCOPE OF THE FUTURE WORK:

The limitation of the present work is that the acceleration feed-back system can't control the static deflection of the boring bar. But high order static deflection can pose problem and result in inaccurate jobs. Displacement feed-back system is capable of controlling the static deflection. So some systems can be thought of which will use the advantages of both the systems ie it will be able to stabilize the system at low feed-back path gain as well as capable of controlling the static deflection actively. Those advantages can be included in a double channel system. First channel will take care of the dynamic deflection and the second one will control the static deflection. A relative displacement sensor will sense the vibration and the corresponding signal will be bifurcated into two paths. First path will include electronic double differentiation circuit and the differentiated signal will be fed to the exciter. Second channel will pass the original signal and only will adjust the D.C biasing in the A.C magnet, according to the change in static voltage level in the displacement sensor due to the static deflection of the boring bar. Due to the presence of the double differentiation circuit the second channel will behave like an acceleration feed-back path and will stabilize at low gain.

Secondly, a modification in the exciter design can also be made. It is seen from the calibration curve of the exciter that it

is more sensitive near the resonance frequency of the boring bar. Though, generally, chatter frequency is near to resonance frequency of the bar, but it sometimes may be bit away from the natural frequency resulting in less sensitivity. The sensitivity of the exciter can be raised in the following way:

A variable capacitor can be connected in series with the magnetic coil and the capacitor can be set to a value where resonance of electrical circuit will occur at chatter frequency. As a result the response will be better and there will be no phase shift between the signal voltage and current.

The analysis of the above theory is given below:

The modified circuit is shown in the fig. [4.16]

The circuit equations are

$$\begin{aligned}
 L_{22} \cdot \frac{di_a}{dt} &= R \cdot i_b = v_1 \\
 \frac{q}{c_1} &= v_2 \\
 i &= \frac{dq}{dt} = i_a + i_b \\
 v &= v_1 + v_2
 \end{aligned}
 \tag{4.1}$$

In laplace domain equation (4.1) becomes

$$L_{22}s.I_a(s) = R.I_b(s) = V_1(s)$$

$$Q(s) = c_1.V_2(s)$$

$$I(s) = s.Q(s) = I_a(s) + I_b(s)$$

$$V(s) = V_1(s) + V_2(s)$$

(4.2)

From (4.1) & (4.2) we get

$$V(s) = R.I_b(s) + \frac{I(s)}{s.c_1} \quad (4.3)$$

Again

$$R.I_b(s) = L_{22}s.I_a(s) \quad (4.4)$$

and

$$I_a(s) + I_b(s) = I(s) \quad (4.5)$$

Solving (4.4) & (4.5) we get

$$I_b(s) = \frac{I(s)}{\frac{R}{L_{22}s} + 1} \quad (4.6)$$

Thus

$$I(s) = \frac{[R.c_1.s + L_{22}c_1.s^2].V(s)}{R.L_{22}c_1.s^2 + R + L_{22}s} \quad (4.7)$$

In the frequency domain (4.7) becomes

$$\frac{I(j.\omega)}{V(j.\omega)} = \frac{R.c_1.j.\omega - L_{22}c_1.\omega^2}{R(1 - L_{22}c_1.\omega^2) + j.L_{22}\omega} \quad (4.8)$$

Putting imaginary part of the r.h.s of the equation (4.8) equal to zero we get the resonance condition and resonance frequency is given by

$$\omega_0 = \left[\frac{R^2}{R^2.L_{22}c_1 - L_{22}^2} \right]^{1/2}$$

When ω_0 is the chatter frequency and it is fixed for a particular cutting condition

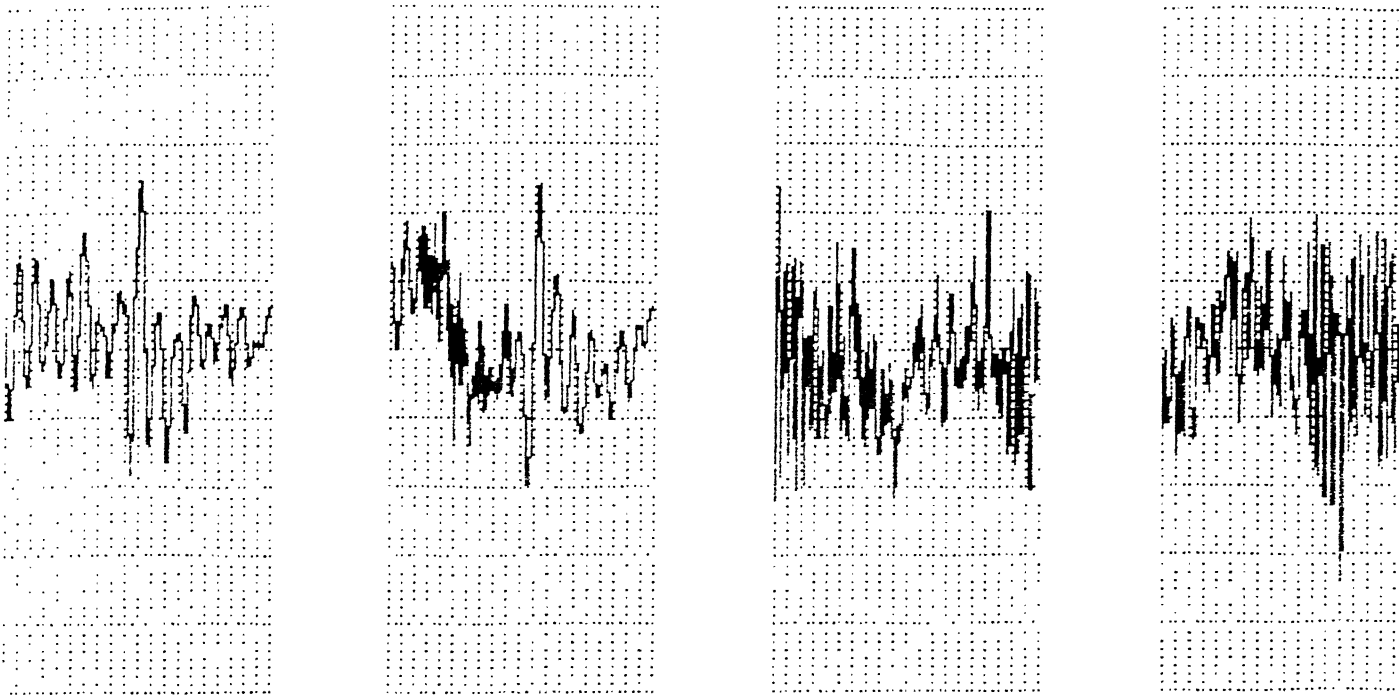
$$c_1 = \frac{R^2 + L_1^2 . \omega_0^2}{R^2 . \omega_0^2 . L_1}$$

will bring the resonance condition of the electrical circuit.

It can be shown that during resonance current will be more in the coil ,than in the previous inductive coil for a fixed voltage level. Consequently more excitation will be available from the exciter.

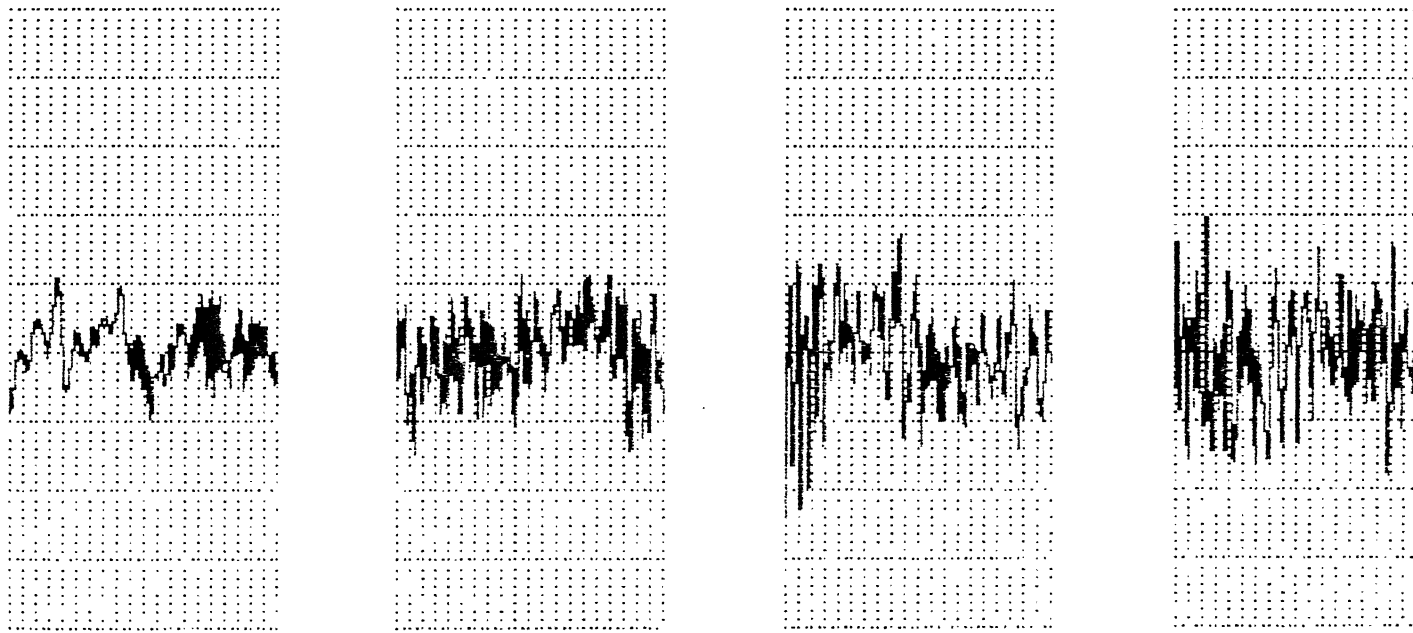
At resonance peak value of current is

$$I = c_1 . R^{3/2} . L_{22}^{-1} . V$$



VIBRATION PATTERN FOR THE UNCONTROLLED CUTTING

Fig. 4.1 spindle rpm =160, feed=0.03mm/rev, width of cut=3mm.



VIBRATION PATTERN FOR THE CONTROLLED CUTTING

Fig. 4.2 spindle rpm =160, feed=0.03mm/rev, width of cut=3mm.
amplifier gain= 6.6×10^{-1}

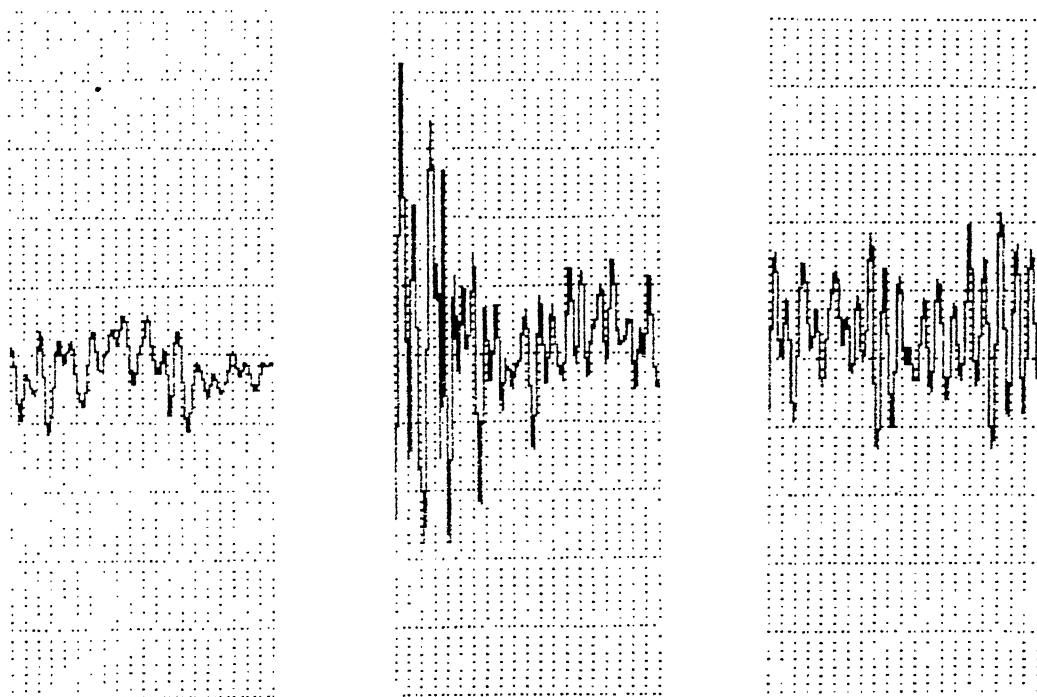


Fig. 4.3 VIBRATION PATTERN FOR THE UNCONTROLLED CUTTING
spindle rpm = 64, feed = 0.046 mm/rev, width of cut = 3 mm.

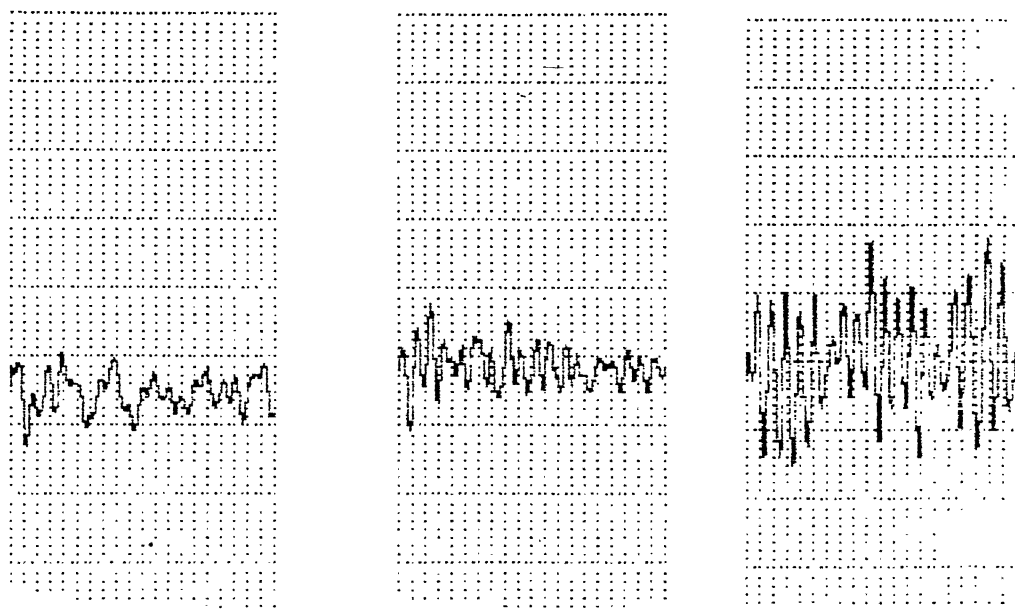


Fig. 4.4 VIBRATION PATTERN FOR THE CONTROLLED CUTTING
spindle rpm = 64, feed = 0.046 mm/rev, width of cut = 3 mm.
amplifier gain = 6.6×10^{-1}

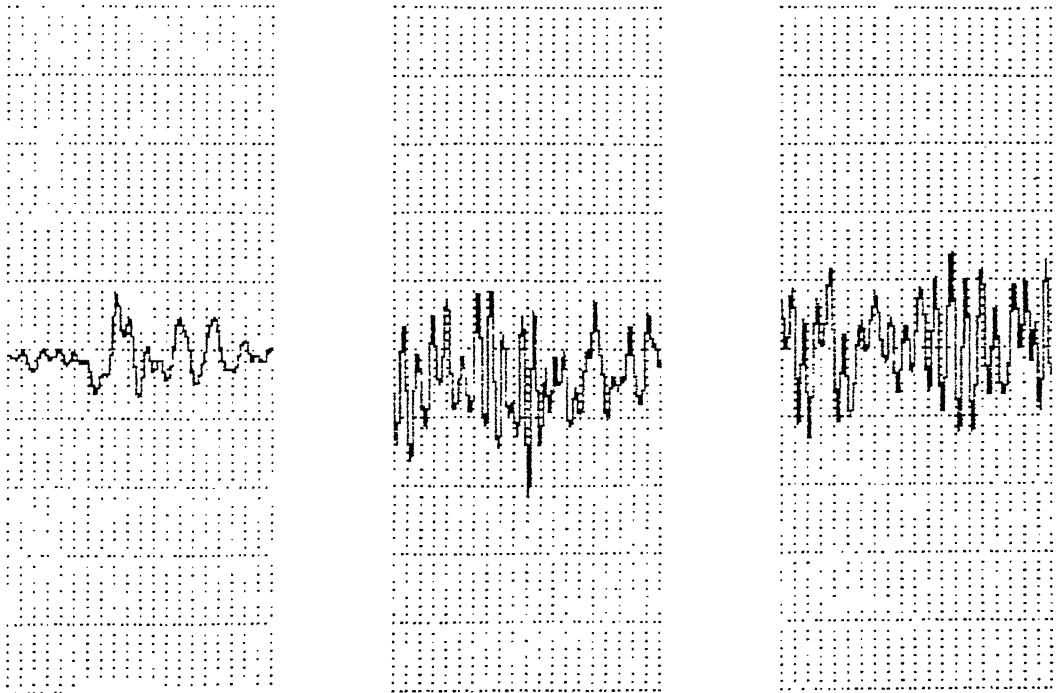
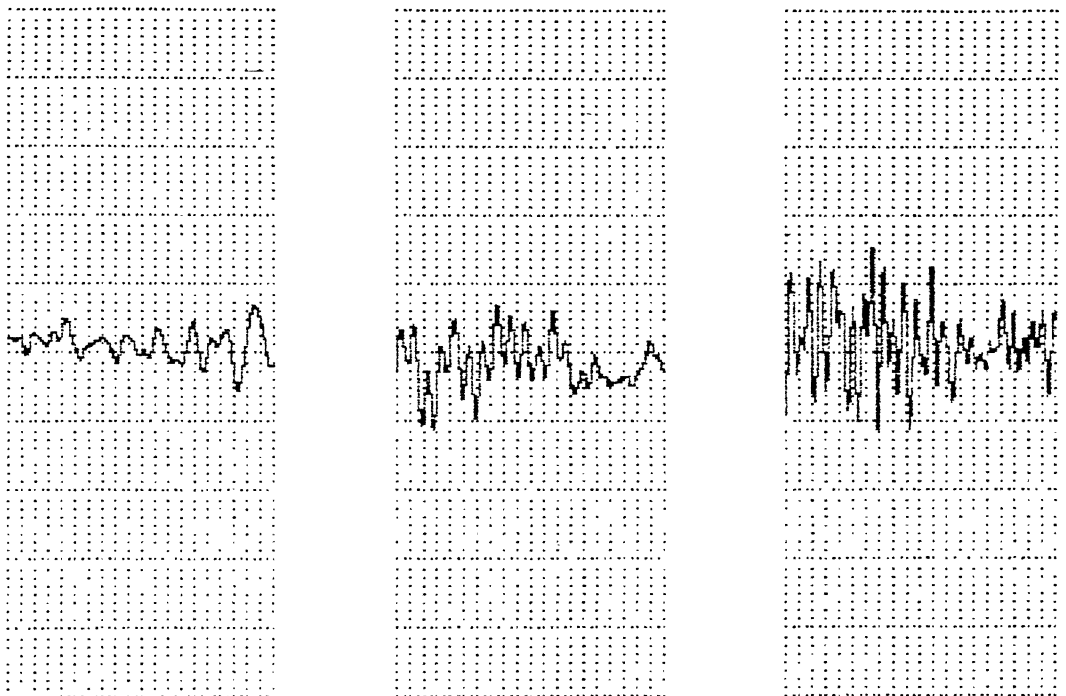


Fig. 4.5 VIBRATION PATTERN FOR THE UNCONTROLLED CUTTING
 spindle rpm =64, feed=0.092mm/rev,width of cut=3mm.



VIBRATION PATTERN FOR THE CONTROLLED CUTTING
 Fig. 4.6 spindle rpm =64, feed=0.092mm/rev,width of cut=3mm
 amplifier gain= 6.6×10^{-1}

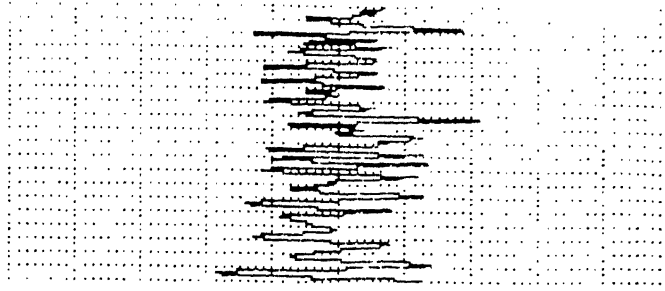
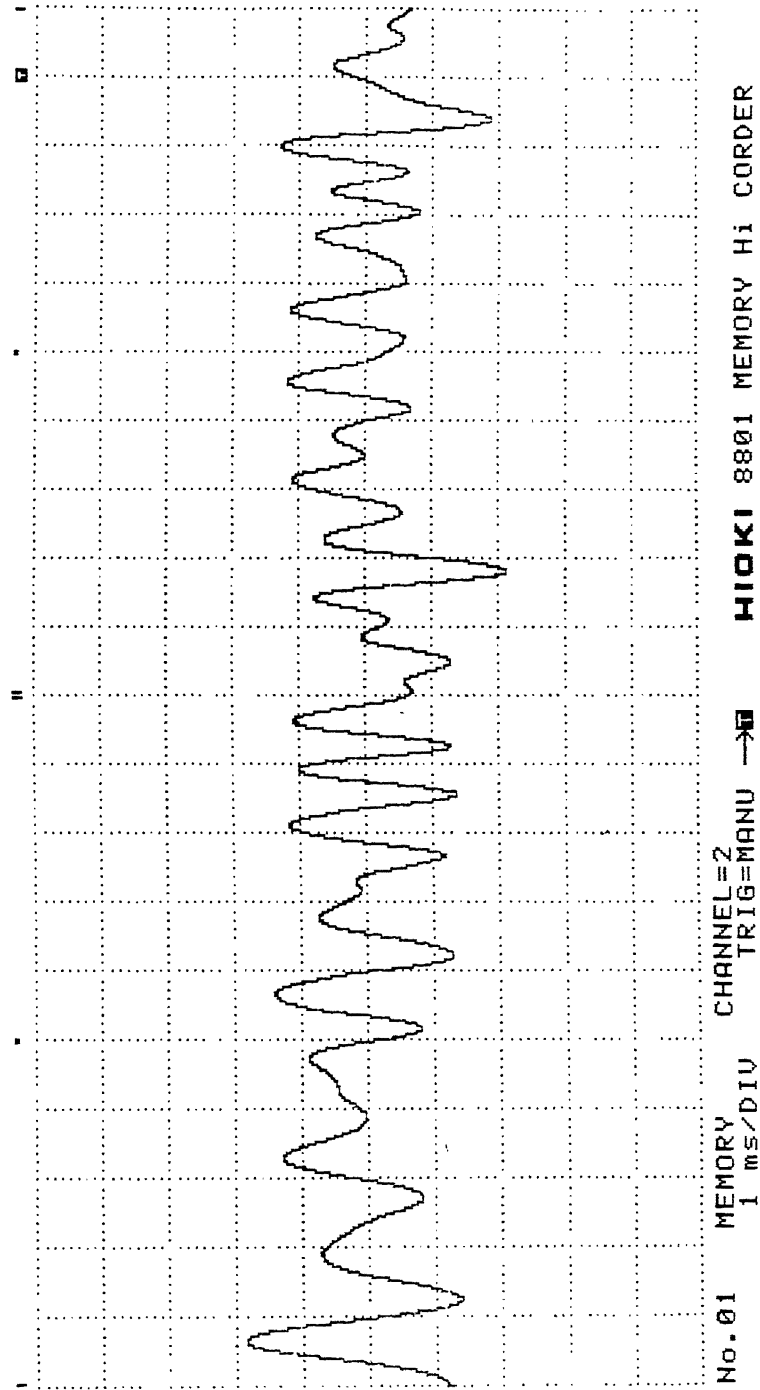
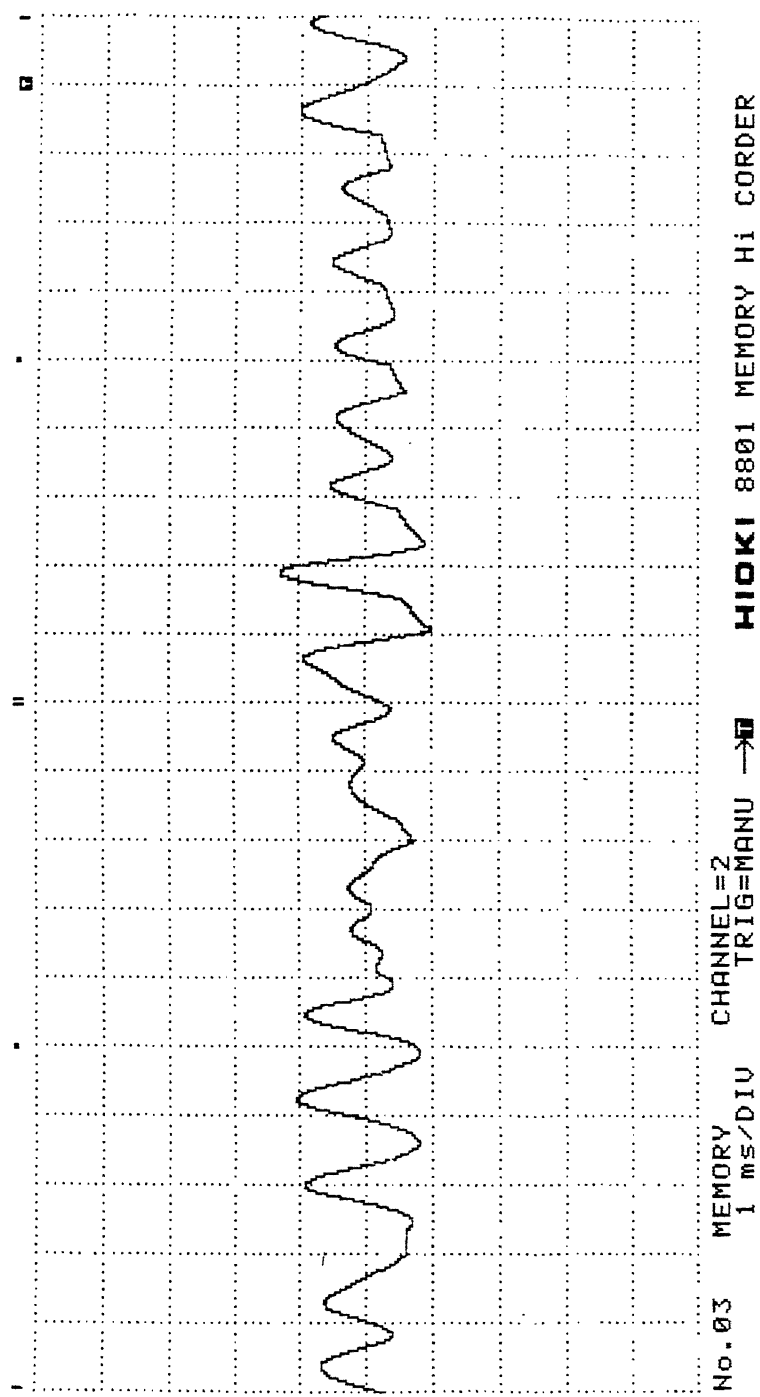


Fig. 4.7 VIBRATION PATTERN FOR THE UNCONTROLLED CUTTING
 spindle rpm =40, feed=0.03mm/rev, width of cut=3mm.



VIBRATION PATTERN FOR THE CONTROLLED CUTTING
 spindle rpm =40, feed=0.03mm/rev,width of cut=3mm.
 amplifier gain= 6.6×10^{-1}

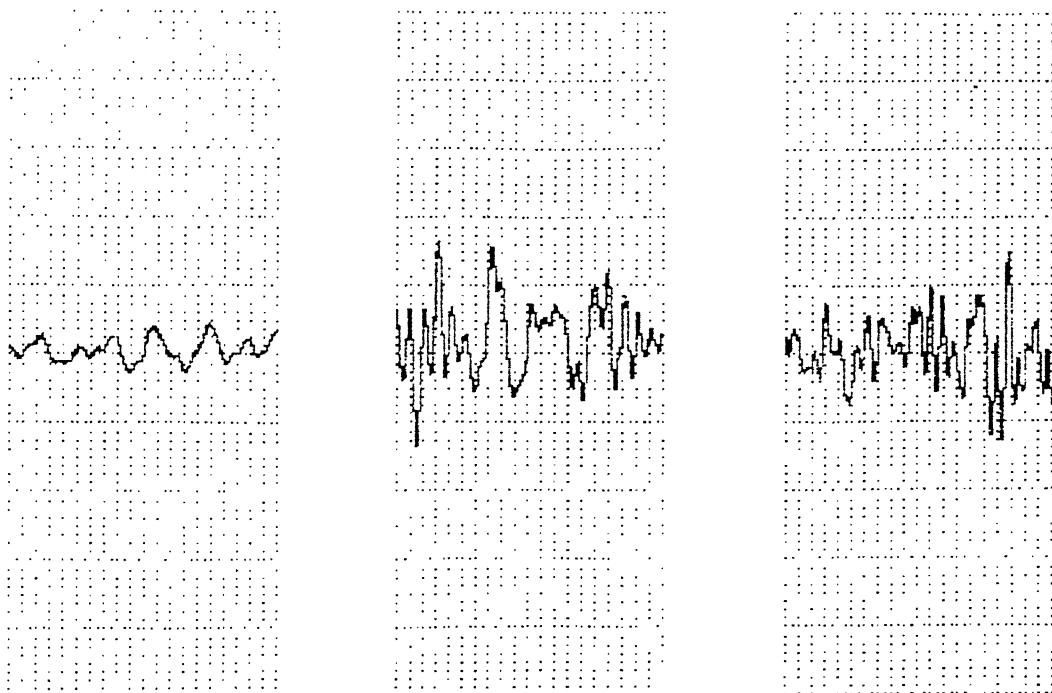
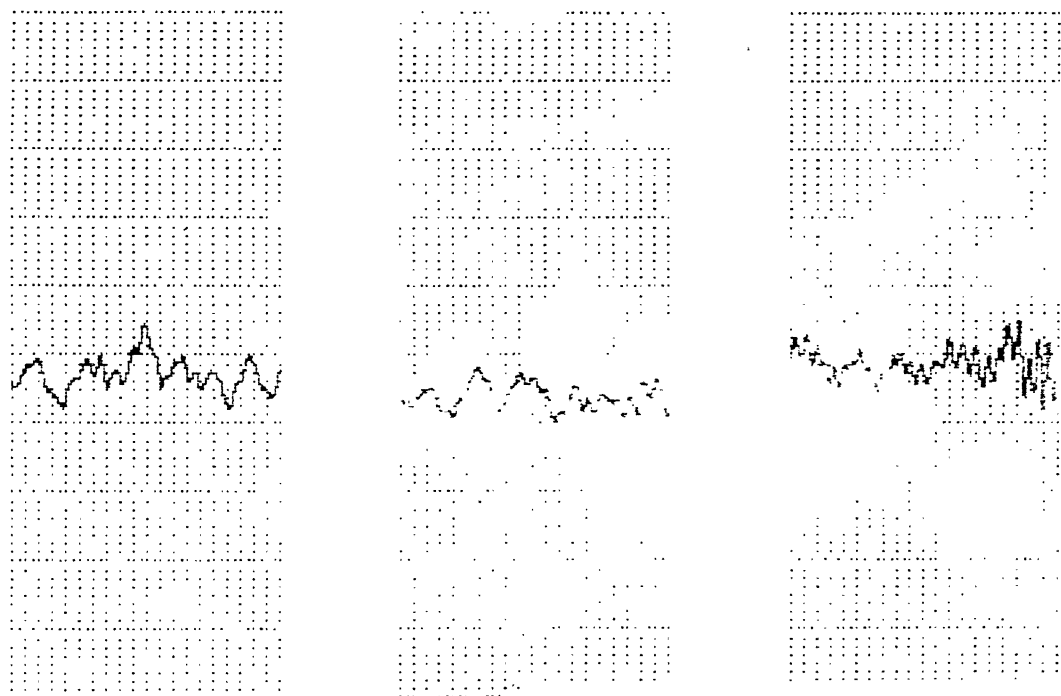
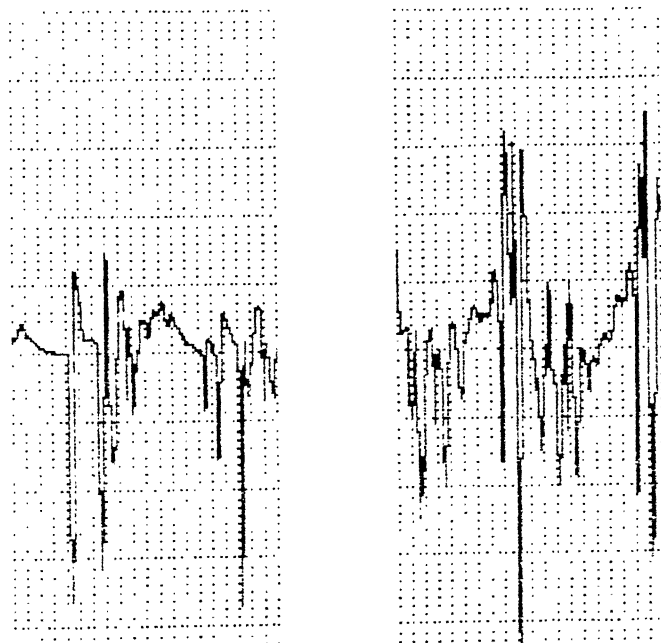


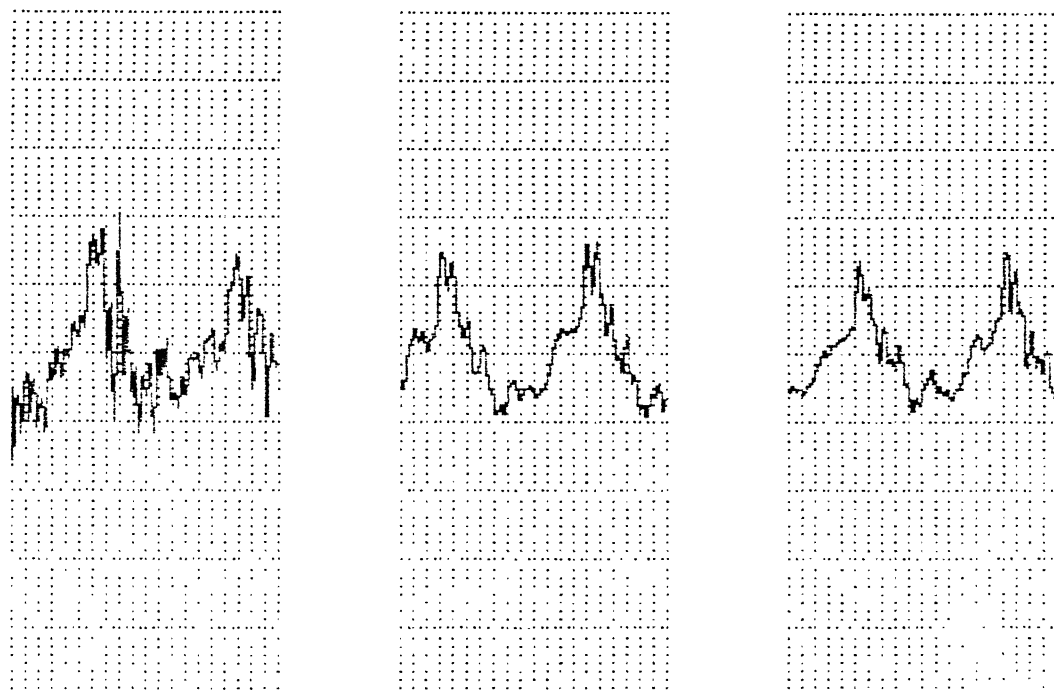
Fig. 4.9 VIBRATION PATTERN FOR THE UNCONTROLLED CUTTING
spindle rpm = 40, feed = 0.075 mm/rev, width of cut = 3 mm.



VIBRATION PATTERN FOR THE CONTROLLED CUTTING
Fig. 4.10 spindle rpm = 40, feed = 0.075 mm/rev, width of cut = 3 mm.
amplifier gain = 6.6×10^{-1}



VIBRATION PATTERN FOR THE UNCONTROLLED CUTTING
 Fig. 4.11 spindle rpm = 320, feed = 0.03 mm/rev, depth of cut = 0.1 mm.



VIBRATION PATTERN FOR THE CONTROLLED CUTTING
 Fig. 4.12 spindle rpm = 320, feed = 0.03 mm/rev, depth of cut = 3 mm.
 amplifier gain = 6.6×10^{-1}

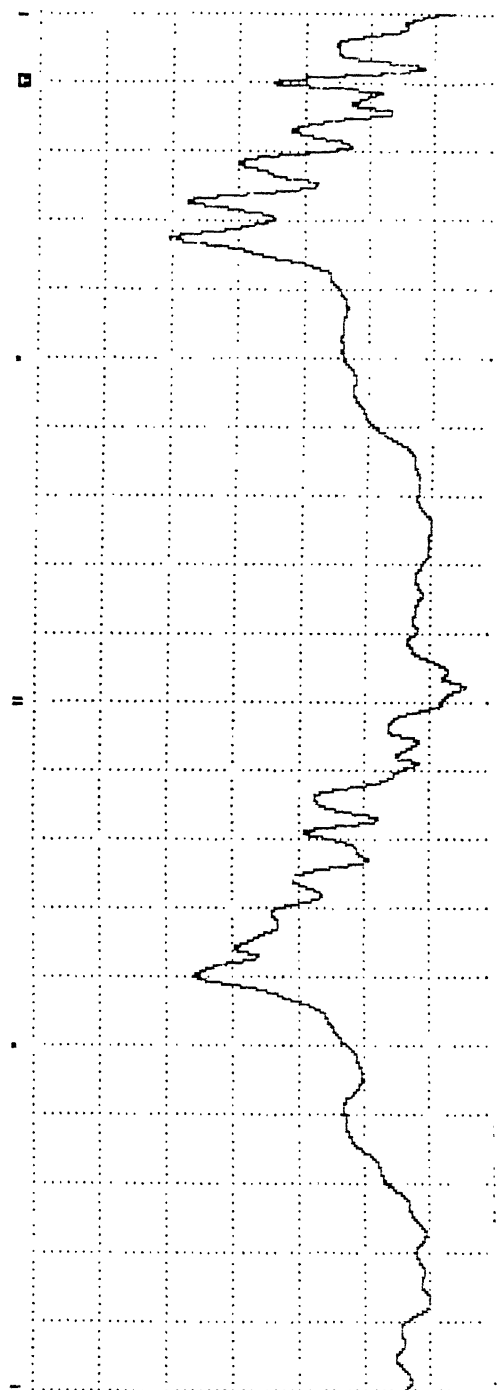


Fig. 4.13 VIBRATION PATTERN FOR THE UNCONTROLLED CUTTING
spindle rpm = 500, feed = 0.03mm/rev, depth of cut = 3mm.

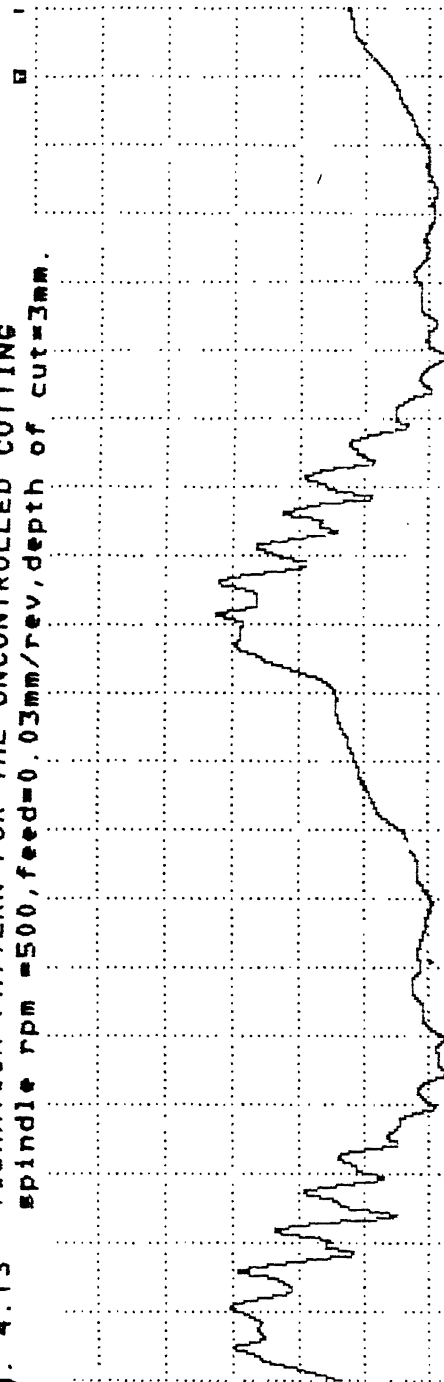


Fig. 4.14 VIBRATION PATTERN FOR THE CONTROLLED CUTTING
spindle rpm = 500, feed = 0.03mm/rev, depth of cut = 3mm.
amplifier gain = 6.6×10^{-4}

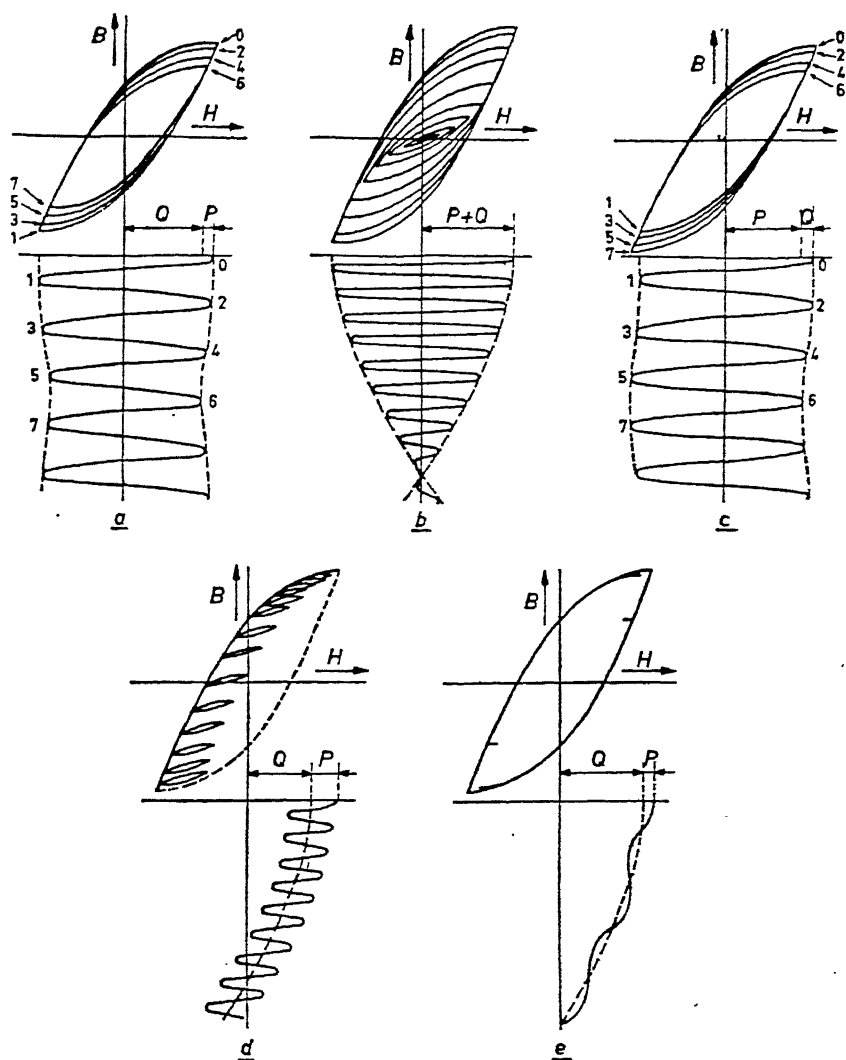


Fig. 4.15 Different examples of hysteresis loops in which the field strength consists of two components of different frequency and different amplitudes.

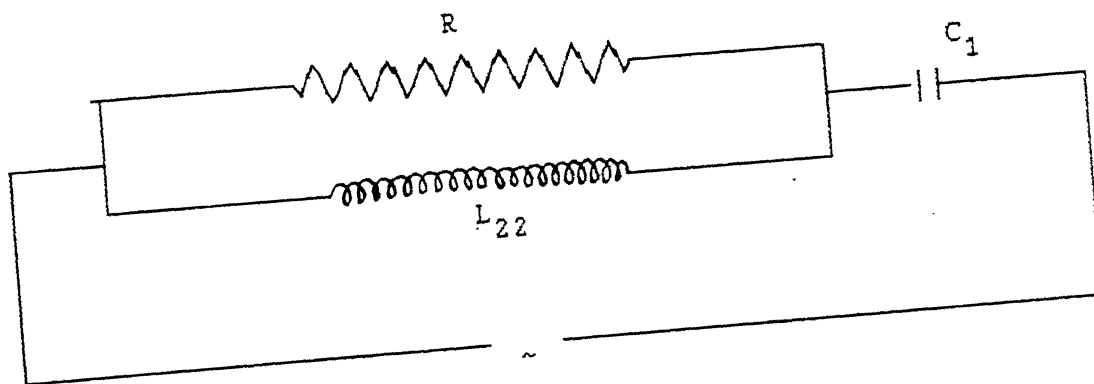
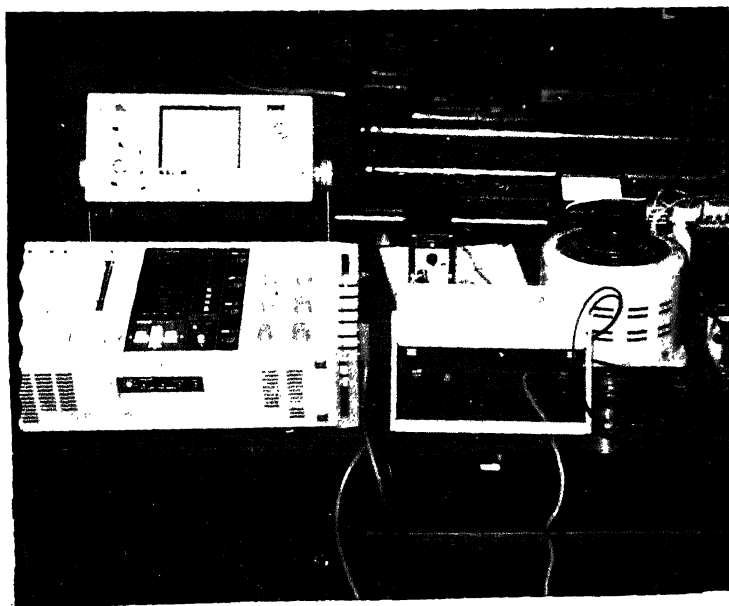


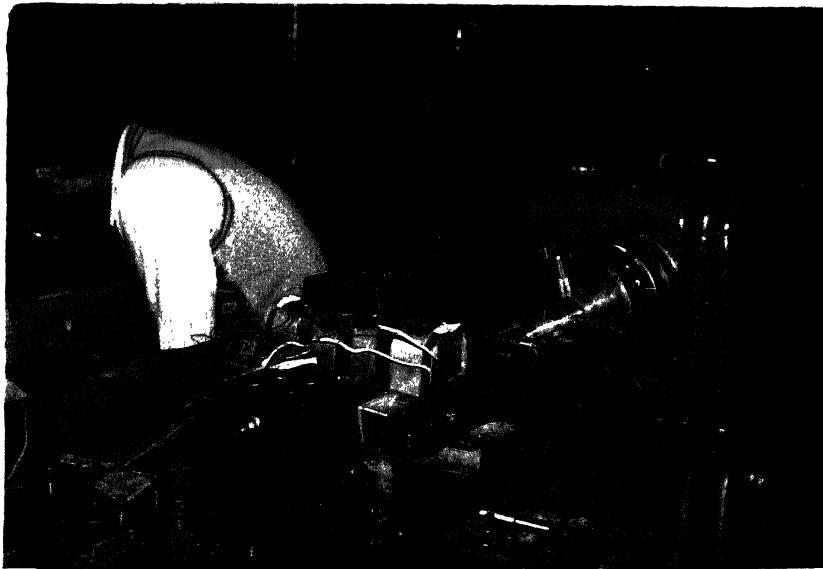
Fig. 4.16 MODIFIED CIRCUIT DIAGRAM OF THE MAGNETIC COIL
FOR IMPROVED RESPONSE OF THE EXCITER



PHOTOGRAPH OF THE EXPERIMENTAL CONTROL CIRCUIT



PHOTOGRAPH OF THE EXPERIMENTAL SET-UP



PHOTOGRAPH OF THE EXPERIMENTAL BORING-BAR

PHOTOGRAPH OF THE EXPERIMENTAL CONTROL CIRCUIT

PHOTOGRAPH OF THE EXPERIMENTAL SET-UP

PHOTOGRAPH OF THE EXPERIMENTAL BORING-BAR

REFERENCES

1. MacManus, B. R., 'A CLOSED LOOP STABILIZATION TECHNIQUE ELIMINATING MACHINE TOOL CHATTER', Int. J. Mach. Tool Des. Res., Vol. 9, pp-197-214.
2. Comstock, T. R.; Tse, F. S. and Lemon, J. R., 'APPLICATION OF CONTROLLED MECHANICAL IMPEDANCE FOR REDUCING MACHINE TOOL VIBRATION', Journal of Engg for Industry, Nov. 1969/1057.
3. Nachtigal, C. L. and Cook, N. H., 'ACTIVE CONTROL OF MACHINE TOOL CHATTER', Transactions of ASME, Journal of basic Engg, p. 236/June 1970.
4. Beilin, L. P., 'DESIGN OF SYSTEMS FOR STABILIZING THE FORCE PARAMETER WHEN CUTTING', Stanki Instrument, Vol. 45, issue 8, 1974, pp7-10.
5. Gorodetskii, M. S., 'GENERAL REQUIREMENTS OF ADAPTIVE SYSTEMS ON LATHES FOR STABILIZATION OF FORCE PARAMETERS DURING CUTTING', Stanki Instrument, Vol. 45, issue 8, 1974, pp 4-7.
6. Klein, R. G.; Nachtigal, C. L., 'A THEORETICAL BASIS FOR ACTIVE CONTROL OF A BORING BAR OPERATION', Transactions of the ASME, Journal of dynamic systems, measurements, and control, June 1975/172.
7. Klein, R. G.; Nachtigal, C. L., 'THE APPLICATION OF ACTIVE CONTROL TO IMPROVE BORING BAR PERFORMANCE', Transactions of the ASME, Journal of dynamic systems, measurements, and control, June 1975/179.
8. Matsubara, Tomio; Yamamoto, Hisataka and Mizumoto, Hiroshi, 'STUDY ON REGENERATIVE CHATTER VIBRATION IN BORING OPERATION (1st REPORT)-INFLUENCE OF DIRECTIONALITY OF BORING BAR ON CHATTER STABILITY', Bull. Japan Soc. of prec. Engg, Vol-23, No. 1 (March 1989).
9. Nachtigal, C., 'DESIGN OF FORCE FEED-BACK CONTROL SYSTEM', Journal of dynamic systems, measurements, and control, March 1972/5.
10. Olsen, E., APPLIED MAGNETISM, 'A STUDY IN QUANTITIES', 1968 Philips technical library.
11. Say, M. G., 'INTRODUCTION TO THE UNIFIED THEORY OF ELECTROMAGNETIC MACHINES', 1971, Pitman publishing.
12. Srinivasan, K.; nachtigal, C., 'APPLICATION OF REGENERATION SPECTRUM IN THE STABILITY ANALYSIS OF MACHINE TOOL CHATTER', Journal of dynamic systems, measurements and control, March 1978/5.

APPENDIX-A

Mode-coupling effect is one of the primary causes of the instability in the cutting process and elastic system during machining operation. Coupled oscillation arises due to the presence of variability of the rigidity of the tool in different directions. In case of a boring bar, this variation in rigidity may be due to difference in clamping force in different directions or asymmetry in tool geometry etc. Two orthogonal modes of vibration will be generated and may be coupled, effecting the instability in the cutting process and the elastic system. This particular cause of instability can be reduced by properly orienting the tool, i.e. the modes, at least up to a satisfactory level. It can be shown that in the absence of regeneration and primary chatter the system will never be unstable due to the sole effect of mode-coupling, if it is ensured by proper designing that the direction of minimum stiffness axis lies outside the angle formed by the normal to machined surface and the instantaneous cutting force vector.

Suppose the rigidity ellipse of the tool has minor axis along x_1 direction and major axis along x_2 direction, as shown in Fig. [A-1]. The vibration along the chip thickness direction is always of major importance.

Equations of motion along x_1 and x_2 directions are written as:

$$\begin{aligned} m_1 \ddot{x}_1 + k_1 x_1 &= f(t) \cdot \cos(\beta - \alpha_1) \\ m_2 \ddot{x}_2 + k_2 x_2 &= f(t) \cdot \cos(\beta - \alpha_2) \end{aligned} \quad (a-1)$$

cutting force $f(t)$ can be formulated as :

$$f(t) = K'_c \cdot \delta u(t) - K'_d \cdot \dot{y}(t) \quad (a-2)$$

change in chip thickness

$$\delta u(t) = - \left[y(t) - \mu \cdot y(t-T) \right] \quad (a-3)$$

Motion along y-direction can be obtained as (fig. A-2)

$$y = x_1 \cdot \cos(\alpha_1) - x_2 \cdot \sin(\alpha_1) \quad (a-4)$$

again

$$\begin{aligned} \alpha_1 &= \alpha_2 - 90^\circ \\ x &= x_1 \cdot \sin(\alpha_1) + x_2 \cdot \cos(\alpha_2) \end{aligned} \quad (a-5)$$

Now, if α_1 is made zero,

$$y = x_1$$

$$x = x_2$$

Then the equation of motion along chip thickness direction ie in the y-direction becomes

$$m \cdot \ddot{y} + k_1 \cdot y = \left\{ K'_c \cdot \left[-y(t) + \mu \cdot y(t-T) \right] - K'_d \cdot \dot{y}(t) \right\} \cdot \cos(\beta) \quad (a-6)$$

or

$$m \cdot \ddot{y} + K'_d \cdot \cos(\beta) \cdot \dot{y}(t) + (k_1 + K'_c \cdot \cos(\beta)) \cdot y(t) + K'_c \cdot \mu \cdot \cos(\beta) \cdot y(t-T) = 0$$

Considering system damping the equation (a-6) is modified to

$$m \cdot \ddot{y} + (C + K'_d) \cdot \dot{y}(t) + (k_1 + K'_c) \cdot y(t) = 0 \quad (a-7)$$

for $\mu=0$ ie in case no regeneration exists,

$$\text{where } K_c = K'_c \cdot \cos(\beta)$$

$$K_d = K'_d \cdot \cos(\beta)$$

Equation (a-7) reveals that the tool motion is not unstable until and unless $C + K_d < 0$, which is generally not satisfied in practice.

Thus one may deliberately create two distinct degrees of freedom by using a side cut boring bar and orient it by making $\alpha_1 = 0$, to avoid mode-coupling. Instead of using side cut boring bar a cylindrical boring bar might have been used, but in that case, if mode-coupling occurs due to uneven clamping force, it is very difficult to detect the exact orientations of the modes and hence it's remedy.

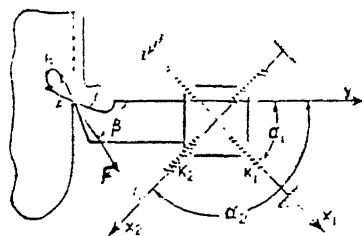


Fig. A-1
 . Tingy's model of a two-degree
 of freedom system

Fig. A-1

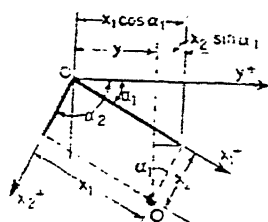


Fig. A-2
 . Co-ordinate relations
 for two-degree motion

Fig. A-2

APPENDIX-B

It is seen that for ferromagnetic materials the magnetization curve (fig.[B-1]) is nonlinear. In the theory it has been taken that permeability is a constant parameter, which implies that the flux ϕ_1 and the current i vary sinusoidally when applied voltage v also varies sinusoidally. Taking nonlinear magnetization characteristics of core into consideration it can be shown that the waveform of current i cannot be sinusoidal even when flux varies sinusoidally. Flux varies sinusoidally when the voltage also varies in the same fashion. However, as shown in the fig.[B-2] flux is a nonlinear function of current, so that current variations associated with a sinusoidal flux variation must be obtained graphically by utilizing the hysteresis loop. In the fig[B-3] current is seen to be non-sinusoidal and peaks when flux is maximum. The distortion in the current is due to the nonlinearity in the magnetization curve. The current peak can reach an abnormally high value if applied voltage is too large and drives the core into saturation. In some circumstances, the harmonics introduced by the distorted current can be troublesome.

It is seen that magnetization curve is mostly nonlinear near low and high values of magneto motive force, with fairly linear region in between. Applying a signal current centered about zero will produce a severely distorted flux density in the core. One can make use of the linear region by applying a fixed magnetization force, a so called D.C bias, which brings the operating point halfway up the linear part as shown in the fig.[B-4].

But a D.C decreases the inductance. Fig.[B-5] shows a large

magnetizing force H_0 present, corresponding to the large D.C current. The alternating current about the constant current sweeps out a minor loop centered about H_0 . The incremental permeability is defined as the average slope of the minor loop:

$$\text{ie } \mu_{inc} = \frac{\Delta B}{\Delta H}$$

The A.C component, thus, experiences an inductance, given by

$$L_1 = \frac{N^2 \cdot A_c \cdot \mu_{inc}}{l_c}$$

Fig.[B-6] shows the variation in minor hysteresis loop when alternating component of the current is kept the same but D.C component is increased. Since the slope of the minor loops decreases it can be concluded that the μ_{inc} decreases as D.C biasing current increases.

The decrease in inductance has two contradictory effects on the exciter dynamics. The reduced inductance will decrease the phase offset between the voltage and current in the coil, but on the other hand will elevate the reluctance of the magnetic circuit (in the analysis the reluctance of the metallic part has been neglected compared to that of the air gap.).

In ferromagnetic materials the relation between magnetic induction (B) and magnetic field strength (H) is nonlinear, while in addition it also encounters hysteresis. In magnetism there are two types of lags, namely 'hysteresis' and 'after effect'. To explain the difference between these two effects (fig.[B-7]) may be considered.

By a small alteration $+\Delta x$ one gets condition B, where y is changed by Δy_1 . If the variation $-\Delta x$ is applied a tB, point A' is

reached via a change $-\Delta y_2$ where $\Delta y_2 < \Delta y_1$.

After a certain time $\Delta y_1 = \Delta y_2$, and this effect is called 'after effect'. If even after a long time, $\Delta y_2 < \Delta y_1$, it is called 'hysteresis'. In magnetic hysteresis the induction thus not only depends on the field strength but also on the magnetic history.

If the material is subjected to slowly-increasing field, the resulting curve showing the relation between B and H is named virgin curve. If an alternating field is superimposed on the static field, one obtains 'an hysteretic state' (fig. [B-8]).

It has been proved that in a coil with a ferromagnetic core one has to reckon with losses. The losses both in the windings and in the core can be considered to be caused by resistances.

The complex impedance Z of the coil can be represented as a parallel connection and

$$\frac{1}{Z} = \frac{1}{R_p} + \frac{1}{j \cdot \omega \cdot L_p}$$

The tangent of the loss angle δ is given by

$$\tan \delta = \frac{\omega \cdot L_p}{R_p}$$

One can also write

$$\tan \delta = \tan \delta_w + \tan \delta_c$$

where δ_w is loss angle due to the losses in windings and δ_c represents the loss angle contributed by the core.

These losses can be classified further as:

- a) hysteresis loss
- b) eddy-current loss
- c) residual loss

The partial losses of a core can also be visualized as resistances and in parallel concept the total resistance is given by

$$\frac{1}{R_c} = \frac{1}{R_{hp}} + \frac{1}{R_{ep}} + \frac{1}{R_{rp}}$$

They can also be represented as loss angles,

$$\tan \delta_c = \tan \delta_h + \tan \delta_e + \tan \delta_r$$

where R_{hp}, δ_h = resistance due to hysteresis loss and the corresponding loss angle

subscript e and r represent eddy-loss and residual loss respectively

Complex permeability:

If R_p is the loss resistance of the core alone then

$$\begin{aligned} \frac{1}{Z} &= \frac{1}{R_p} + \frac{1}{j \cdot \omega \cdot L_0 \cdot \mu'_p} \\ &= \frac{1}{j \cdot \omega \cdot L_0} \left(\frac{1}{\mu'_p} + \frac{j \cdot \omega \cdot L_0}{R_p} \right) \end{aligned}$$

where μ'_p represents real permeability of the core

L_0 = inductance of the coil in air

$$\begin{aligned} &= \frac{1}{j \cdot \omega \cdot L_0} \left(\frac{1}{\mu'_p} + \frac{j}{\mu''_p} \right) \\ &= \frac{1}{j \cdot \omega \cdot L_0 \cdot \mu} \end{aligned}$$

By the term 'complex permeability' in parallel terms one understands

$$\frac{1}{\underline{\mu}} = \left[\frac{1}{\underline{\mu}'} + \frac{j}{\underline{\mu}''} \right]$$

p p

Thus ,complex permeability is a function of frequency and consequently the loss angle changes with the frequency .the discussion so far made reveals the fact that B and H need not to be in phase.

Eddy-current losses:

Eddy current losses are produced in all conducting materials when they are situated in an alternating magnetic or electric field.As a rule the eddy current should be kept as low as possible.In order to suppress the eddy losses in iron core ,as much of it as possible,is constructed of thin laminations,which are insulated from one another .

Loss angle for eddy current can be found out to be:

$$\tan \delta_e = \frac{\sinh k_0 - \sin k_0}{\sinh k_0 + \sin k_0}$$

where $k_0 = d \cdot \sqrt{\frac{w \cdot \mu_0}{2 \cdot \rho}}$

where d=thickness of lamination

ρ =specific resistance of core material

core impedance components corresponding to eddy losses are

$$L_p = \frac{2.L_0.\mu_r}{k_0}$$

$$R_p = \frac{2.w.L.\mu_r}{k_0}$$

where $L_0 = \frac{N^2.\mu_0.a.b}{l_c}$

where 'a' is the total stacking height of the core, 'b' is width of the core and l_c is the length of the core, N is the no. of turns in the magnetic coil.

Loss angle due to hysteresis:

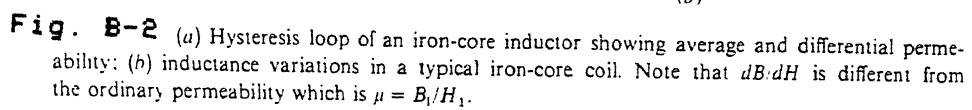
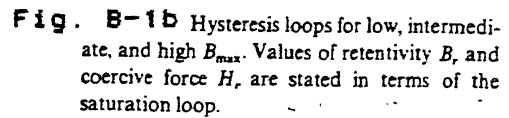
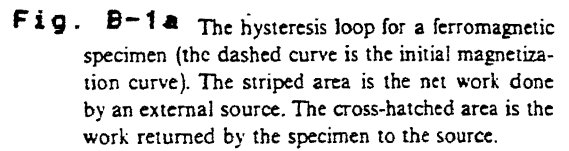
Loss angle δ_h due to hysteresis is given by

$$\tan \delta_h = \frac{4.v.N.\bar{i}}{3.\pi.\mu_a.l_f}$$

where v = coefficient of quadratic factor (assuming hysteresis curve as parabola)

l_f = path of the field lines in cm.

$$\bar{i} = \frac{\sqrt{2}.i}{1000} \quad , \quad i \text{ in mili amps.}$$



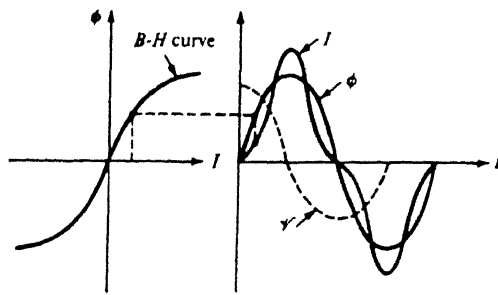


Fig. B-3 Distortion in current I by the nonlinearity of the BH curve.

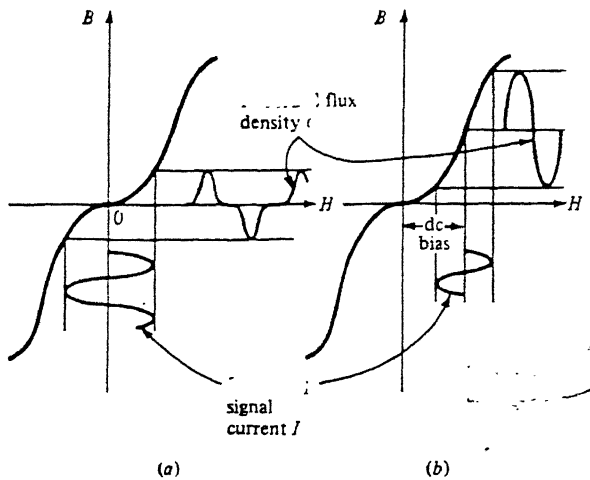


Fig. B-4 (a) The magnetization is not a faithful reproduction of the signal current; (b) linear operation is achieved by the use of dc bias;

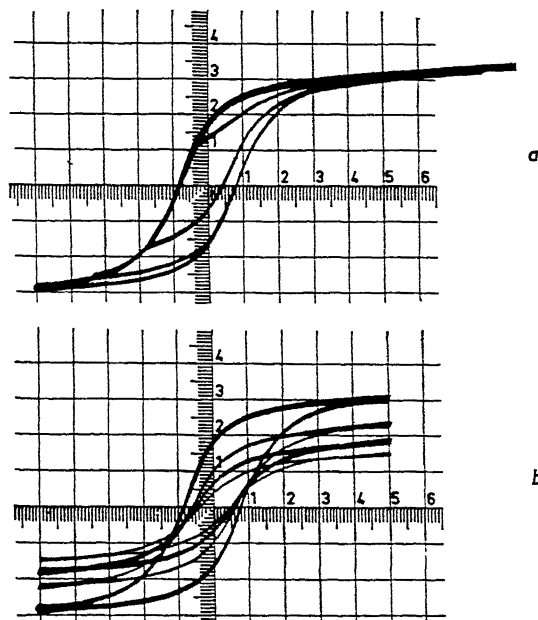


Fig. B-4.1 Hysteresis loops with a biasing field. The static magnetic fields are parallel (a) and perpendicular (b) to the alternating field. The alternating field strength is kept constant.

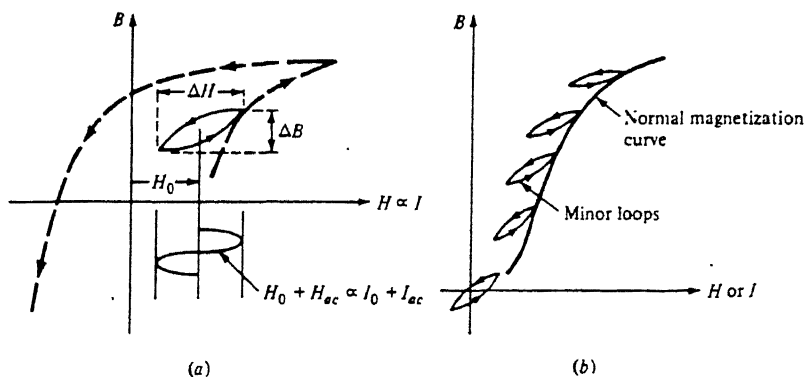


Fig. B-5 (a) Minor hysteresis loop due to superposed direct I_0 and alternating current I_{ac} :
(b) minor loops for different values of direct current.

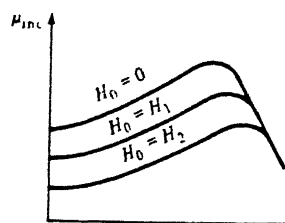


Fig. B-6 Typical incremental permeability versus amplitude of alternating flux density for iron. $H_2 > H_1$.

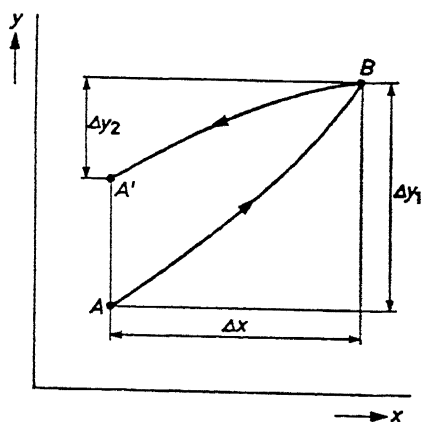


Fig. B-7

APPENDIX-C

The theory of regeneration spectrum in the stability analysis of metal cutting has been introduced by K. SRINIVASAN & C.L. NACHTIGAL [12]. In the present work it has been slightly modified and removal of certain limitations became necessary.

Let the characteristics equation of the system be of the form

$$P(s) - Q(s) \cdot e^{-s \cdot T} = 0$$

There are infinite number of roots of the equation, which can generally be represented by

$$s_{k,-k} = \alpha_k \pm j \cdot \omega_k, \quad k = 1, 2, 3, \dots$$

The characteristics equation can be rearranged as

$$e^{s \cdot T} = \frac{Q(s)}{P(s)} = R(s)$$

putting $s = \alpha_k + j \cdot \omega_k$ in the equation () and taking modulus on both side we get

$$|e^{(\alpha_k + j \cdot \omega_k) \cdot T}| = |R(\alpha_k + j \cdot \omega_k)|$$

or

$$e^{\alpha_k \cdot T} = |R(\alpha_k + j \cdot \omega_k)|$$

The condition of stability requires that

$$\alpha_k \leq 0$$

$$\text{ie } |R(\alpha_k + j \cdot \omega_k)|_{\max} \leq 1, \text{ for stability}$$

In the paper[] it has been stated that the regeneration spectrum (plot of $|R(\alpha_k + j \cdot \omega_k)|$ vs. ω_k) is independent of time delay T, but it has been found that it may not be always true. When penetration resistance is considered in the dynamics of cutting, T

is introduced into the system characteristics equation through K_d , an arbitrary criterion is set in the paper for the validity of the above theory that

$$T \geq \frac{5}{|\alpha_{\max}|}, \text{ where } \alpha_{\max} \text{ is the real part of the least stable}$$

root of the equation $P(s) = 0$. The higher values of t will make the closer spacing of the roots possible and they are so near to imaginary axis, as α_k can be replaced by least stable real part α_0 .

A closer inspection may help in relaxing the above limitations on T and very simple procedure can be adopted to find α_0 .

If α_0 is the least stable real part then obviously

$$e^{\alpha_0 \cdot T} = |R_{\max}(\alpha_0 + j \cdot \omega_k)|_{\omega_i = \omega_0}$$

Plotting $e^{\alpha_0 \cdot T}$ and $R_{\max}(\alpha_0 + j \cdot \omega_k)$ for values of ω in the range $0 < \omega_k < \text{inf.}$, for each value of α_0 in the range $-\text{inf.} < \alpha_0 < +\text{inf.}$ one may find out α_0 and ω_0 when

$$e^{\alpha_0 \cdot T} = |R(\alpha_0 + j \cdot \omega_0)|$$

But $|e^{\alpha_0 \cdot T} - R(\alpha_0 + j \cdot \omega_0)| \leq 0.001$ is sufficient to stop the searching. Obviously α_0 is the chatter growth exponent and ω_0 is the chatter frequency. But chatter may occur at any value of ω , for which value of regeneration amplitude is greater than 1.

Thus the above theory becomes valid for all values of T . The procedure becomes easy with the help of a digital computer.

APPENDIX-D

Let I_h be the current in the magnetic coil corresponding to signal voltage V_h and frequency ω_h . Let for other frequency ω_1 and signal voltage V_1 , I_1 be the current in the coil. Now if $V_h > V_1$ and $\omega_h > \omega_1$ then $I_h < I_1$ condition will be achieved if following condition holds good

$$\frac{V_h \left[\sqrt{(L_{22} \cdot \omega_h)^2 + R^2} \right] \cdot \omega_1}{V_1 \left[\sqrt{(L_{22} \cdot \omega_1)^2 + R^2} \right] \cdot \omega_h} < 1$$

So it is sometimes possible that a low frequency signal even with low signal voltage level can produce greater current than a high frequency and high voltage signal. Consequently a higher degree of excitation in the exciter is possible with a low frequency signal compared to a high frequency input.